The transition from acute to chronic pain: dynamic epigenetic reprogramming of the mouse prefrontal cortex up to 1 year after nerve injury

Lucas Topham[a,b], Stephanie Gregoire[a,b], HyungMo Kang[a,b], Mali Salmon-Divon[c,d,e], Elad Lax[c,d], Magali Millecamps[a,b], Moshe Szyf[d,f], Laura S. Stone[a,b,d,g,h,*]

Abstract

Chronic pain is associated with persistent structural and functional changes throughout the neuroaxis, including in the prefrontal cortex (PFC). The PFC is important in the integration of sensory, cognitive, and emotional information and in conditioned pain modulation. We previously reported widespread epigenetic reprogramming in the PFC many months after nerve injury in rodents. Epigenetic modifications, including DNA methylation, can drive changes in gene expression without modifying DNA sequences. To date, little is known about epigenetic dysregulation at the onset of acute pain or how it progresses as pain transitions from acute to chronic. We hypothesize that acute pain after injury results in rapid and persistent epigenetic remodelling in the PFC that evolves as pain becomes chronic. We further propose that understanding epigenetic remodelling will provide insights into the mechanisms driving pain-related changes in the brain. Epigenome-wide analysis was performed in the mouse PFC 1 day, 2 weeks, 6 months, and 1 year after peripheral injury using the spared nerve injury in mice. Spared nerve injury resulted in rapid and persistent changes in DNA methylation, with robust differential methylation observed between spared nerve injury and sham-operated control mice at all time points. Hundreds of differentially methylated genes were identified, including many with known function in pain. Pathway analysis revealed enrichment in genes related to stimulus response at early time points, immune function at later time points, and actin and cytoskeletal regulation throughout the time course. These results emphasize the importance of considering pain chronicity in both pain research and in treatment optimization.

Keywords: DNA methylation, Chronic pain, Epigenetics, Prefrontal cortex, Time course, Epigenetics, Neuropathic, Animal model

1. Introduction

Chronic pain is a global challenge, affecting between 10% and 20% of adults and costing billions each year in patient care and lost productivity.[21,28,54] Chronic pain is modulated by

a complex mix of biological, psychological, and social factors. At the molecular level, hundreds of genes become differentially expressed in chronic pain conditions.[1,29,37,43,71] Understanding chronic pain is further complicated by time-dependent recruitment of mechanisms and pathways mediating the transition from acute to chronic pain.[12,49] Improved understanding of pathological gene dysregulation from acute to chronic pain is desperately needed to prevent the development of prolonged, intractable pain.

Epigenetic mechanisms allow for malleable and reversible gene regulation without modification of DNA sequences. DNA methylation is an epigenetic regulator of gene expression wherein a methyl group is added to cytosine DNA nucleotides. When methylation occurs in gene promoter regions, the gene is typically repressed through hindrance of transcription factor binding, recruitment of methyl binding proteins, and chromatin remodeling, ultimately preventing RNA polymerase-mediated transcription.[19,32]

DNA methylation is environmentally sensitive, with methylation profiles changing in response to addiction, early life stress, and neurodegenerative disease.[46,52,55] Chronic pain is also associated with changes in DNA methylation in both humans and animal models across many tissues including the prefrontal cortex (PFC), dorsal root ganglia, and spinal cord.[20,22,43,63] DNA promoter methylation at specific genes can be linked to the degree of mechanical hypersensitivity,[43] and chronic treatment with the methyl donor S-adenosylmethionine increased global DNA

methylation in the PFC and attenuated mechanical hypersensitivity.[23] Investigation of DNA methylation's role in chronic pain advances our understanding of pain progression and may reveal potential therapeutic avenues.

Among the structures involved in chronic pain, the PFC is crucial as an integrator of ascending sensory information, cognitive and emotional responses, and descending inhibitory control.[10,36,70] In human patients and animal subjects, long-term pain results in a persistent functional and anatomical reorganization of the PFC,[5,35,57,59] with patients showing more PFC activation than healthy controls.[4,6] Chronic pain patients are commonly comorbid for depressive and anxiety disorders[58] that are heavily correlated with PFC abnormal functioning.[33,51] As a central mediator in the pain pathway, therapeutic mechanisms targeting PFC may have efficacy across different pain disorders and simultaneously address associated cognitive and emotional comorbidities.

Previous work has shown extensive changes in DNA methylation and dynamic structural and functional reorganization in the PFC to be associated with chronic pain. To track epigenetic reprogramming in the PFC in acute and chronic pain, we captured the pattern of genome-wide DNA methylation across time from 1 day to 1 year after peripheral nerve injury in mice. Our analysis revealed a dynamic pattern of DNA methylation across the time course, implicating hundreds of differentially methylated (DM) genes at each time point. Subsequent analysis revealed time point-specific changes that reveal potential underlying mechanisms. Our data show that epigenetic reprogramming occurs early during the transition from acute to chronic pain and is consistent with a potential causal role.

2. Materials and methods

2.1. Animals

78 male CD-1 mice (Charles River Laboratories, St-Constant, QC, Canada) were used in this study. Animals were received at 6 to 8 weeks of age and housed 3 to 4 per cage on a 12-hour light/dark cycle in a temperature-controlled room in ventilated polycarbonate cages (Allentown, Allentown, NJ) with corncob bedding (7097; Teklad Corncob Bedding, Envigo, United Kingdom) and cotton nesting squares for enrichment. Mice were given access to food (2092X Global Soy Protein-Free Extruded Rodent Diet, Irradiated) and water ad libitum. Animals were habituated to the housing conditions for at least one week before any experimental interventions.

Animals designated for DNA methylation analysis were randomly assigned to receive either the spared nerve injury (SNI) model of neuropathic pain or sham surgery control and the model was allowed to develop for one day (D1), 2 weeks (W2), 6 months (M6), or 1 year (1Yr) postinjury. Final numbers per group (Sham/SNI)—D1:4/4; W2:6/6; M6:6/6; 1Yr:4/6; 42 animals in total.

Animals designated for immunohistochemistry were randomly assigned to either SNI or sham surgery and allowed to progress to 2 weeks or 6 months postinjury. Final numbers per group (Sham/SNI)—W2:10/8; M6:10/8; 36 animals in total.

All experiments were approved by the Animal Care Committee at McGill University, and conformed to the ethical guidelines of the Canadian Council on Animal Care and the guidelines of the Committee for Research and Ethical Issues of the International Association for the Study of Pain.[76]

2.2. Induction of spared nerve injury

Nerve injury was induced using the SNI model of neuropathic pain, as adapted for mice[14,60] at 10 to 12 weeks of age. Under deep isoflurane anesthesia, an incision was made on the medial surface of the thigh, exposing the 3 branches of the sciatic nerve. Spared nerve injury surgery consisted of ligation and transection of the left tibial and common peroneal branches of the sciatic nerve, while sparing the sural nerve. The tibial and common peroneal branches were tightly ligated with 6:0 silk (Ethicon, Cincinnati, OH) and sectioned distal to the ligation. Sham surgery consisted of exposing the nerve without damaging it.

2.3. Behavioural assessment of mechanical sensitivity

After a habituation period of 1 hour to the testing environment of Plexiglas boxes placed on a wire mesh grid, von Frey filaments (Stoelting Co, Wood Dale, IL) were applied to the plantar surface of the hind paw to the point of bending for 3 seconds or until withdrawal. Mechanical sensitivity was determined as the 50% withdrawal threshold using the up-down method.[11] The stimulus intensity ranged from 0.04 to 4.0 g, corresponding to filament numbers 2.44 to 4.56. Testers were blind to the condition of the animal.

2.4. Immunofluorescent histochemistry

Animals were deeply anesthetized with an intraperitoneal injection of ketamine (100 mg/kg), xylazine (10 mg/kg), and acepromazine (3 mg/kg). Animals were perfused with 100 mL vascular rinse (0.2M phosphate buffer with sodium nitrate), followed by 200 mL Lana's fixative (4% paraformaldehyde, 14% saturated picric acid, 0.16M phosphate buffer, pH 6.9), and then 100 mL 10% sucrose solution in phosphate buffered saline. Tissue was cryoprotected in 10% sucrose solution at 4°C for 3 days, and then coronally divided at Bregma into forebrain and hind brain sections. Brain tissue was coronally sectioned at 14 μm on a cryostat (Leica), and PFC sections, defined as +1.54 mm to +1.98 mm from Bregma, were collected. Prelimbic and infralimbic areas were defined according to Paxinos and Franklin.[53]

Tissue was incubated with blocking buffer (1% Normal Donkey Serum, 1% Bovine Serum Albumin, 0.3% Triton X-100, 0.01% Sodium Azide) for 1 hour before primary antibody incubation overnight at 4°C. Tissue sections were either singly stained with rabbit anti-NeuN (1:1000, Abcam, Ab177487), or double stained with mouse anti-NeuN (1:1000, Millipore, MAB377) and either rabbit anti-GFAP (1:1000, Neomarkers, RB087AO) or rabbit anti-Iba1 (1:1000, Wako, 019-19741). Rabbit anti-NeuN was used to quantify neuronal cell counts, whereas mouse anti-NeuN was used as a counter stain to define cortical layers in double-stained sections. Secondary antibodies donkey anti-rabbit Alexa 594 (1:200, Jackson ImmunoResearch, 711-585-152) and donkey anti-mouse Alexa 488 (1:200,Jackson ImmunoResearch, 714-545-150) were incubated for 90 minutes at room temperature. Sections were counterstained with DAPI (4′,6-diamidino-2-phenylindole, 1:50000, Sigma, D9542) and coverslipped with AquaPolymount (18606, PolySciences).

2.5. Immunohistochemistry quantification

FIJI[56] and manual cell counting were used to quantify the number of total cells, neurons, astrocytes, and microglia in prelimbic and infralimbic brain areas. DAPI was used as a marker of total cell population, NeuN-immunoreactivity (-ir) defined neuronal

populations, GFAP-ir defined astrocyte populations, and Iba1-ir defined microglial populations. NeuN staining was also used to separately designate layer I, superficial (layers II-III), and deep (layer V) cortical layers to aid the placement of 3 regions-of-interest (ROIs) per layer. Cell quantification was based on colocalization of the cell type-specific marker with DAPI, and cell counts were averaged across 3 ROIs per layer. The averaged ROI area per cortical layer: layer I: 6724 μm^2; superficial (layers II-III): 15,790.14 μm^2, deep (layer V): 10,526.76 μm^2. An overall cell count was calculated by adding the counts from all 3 layers. Total ROI area: 33,040.9 μm^2. Regions-of-interest sizes were identical between prelimbic and infralimbic areas.

2.6. Isolation of prefrontal cortex, DNA capture, and bisulfite sequencing

Mouse PFC was dissected after isoflurane anesthesia and decapitation. Prefrontal cortex was defined as a region with an anterior boundary of the frontal pole, approximately +3.00 Bregma, posterior boundary of +1.42 Bregma, lateral boundaries of +1 mm from midline, and a ventral boundary wherein the olfactory bulb, caudate putamen, and areas below the rhinal fissure and lateral ventricles were all removed.[53] This defined area isolates the prelimbic, orbital, and infralimbic cortices corresponding to the mouse medial PFC. Once dissected, tissue was homogenized and genomic DNA was extracted using the Qiagen DNeasy Blood and Tissue kit and protocol.

Genome-wide methylation analysis was performed using the Roche SeqCap Epi Developer M Enrichment system on bisulfite-treated DNA (Roche Nimblegen, Madison, WI), with custom-designed primers targeting promoter and enhancer regions of the genome. Probe design was based on the mm9 reference genome and associated H3K4me1 and H3K4me3 binding (probe BED file available in Supplemental Table 1, available at http://links.lww.com/PAIN/B21). Briefly, 1 μg of genomic DNA per sample was fragmented into 200 bp lengths, and adapter and index sequences were ligated to each end of the fragment according to the KAPA Library Preparation Kit protocol. Sample DNA was then bisulfite converted following the EZ DNA Methylation-Lightning Kit (Zymo Research, CA). Sample DNA was then PCR amplified, hybridized with custom capture probes, and PCR amplified again in accordance with Roche SeqCap Epi system protocols.[69] Sample captured bisulfite-converted DNA sequencing was performed by Genome Quebec on the Illumina HiSeq 2500 following Illumina guidelines. Paired-end sequencing reads of 125bp in length were generated.

2.7. DNA methylation preprocessing

Capture sequencing data were preprocessed using the McGill University Genome Quebec Innovation Centre GenPipes Methyl-Seq Pipeline.[8] The pipeline proceeds through Trimmomatic, Bismark Align, Picard Deduplication, and Bismark Methylation Call.[7,34] Baseline pipeline parameters were set as a minimum sequence quality of PHRED score >30, alignment reference genome was mm10 (GRCm38), and minimum read coverage per base was set at 10 reads. A detailed outline of the Methyl-Seq pipeline steps and process can be found at https://bitbucket.org/mugqic/genpipes. Before analysis, collected sequence data were filtered to remove a blacklist of regions identified to have anomalous, unstructured, and high signal/read counts in next-gen sequencing.[2] The blacklist used was specific for mm10 and the BED file can be found in Supplemental Table 2 (http://links.lww.com/PAIN/B22).

2.8. Differential methylation analysis

Generalized linear model analysis was used to compare Sham to SNI methylation values at each time point. Differential methylation analysis was performed using R and the edgeR package.[13] Samples were normalized to library size, where library size was set to be the average of the total read counts for methylated and unmethylated CpGs. For a CpG site to pass through to analysis, it was required to be sequenced at a depth of at least 10 reads in each sample within a time point.

At each time point, CpGs were defined as being DM if the false discovery rate (FDR) was less than <0.1 and a difference in methylation between Sham and SNI of >5%. Although the selection of an FDR threshold of 0.1 carries greater risk of type I error than the more typical threshold of 0.05, it is preferable for the exploratory purposes of this study. Differential methylation between Sham and SNI was determined by calculating the M-Value (log_2 of the ratio [methylated cytosines/unmethylated cytosines]) of each CpG site in Sham and SNI, and then detecting statistically significant differences. The methylation percentage (percentage of [methylated cytosines/total cytosines]) at each site was also calculated. Differentially methylated samples were further divided into hypermethylated CpGs or hypomethylated CpGs with the Sham CpG methylation percentage acting as the reference point. If the SNI CpG methylation is 5% or larger than the Sham, the CpG position is considered to be hypermethylated. If the SNI CpG methylation is reduced by −5% or more compared to Sham, the CpG position is considered to be hypomethylated.

CpGs were annotated to their associated genes and genomic regions using the topTags function of edgeR[13] and annotatePeaks function of the ChIPseeker[73] R packages, using a TxDb object created from the Gencode "mmusculus_gene_ensembl" Biomart database. Each CpG position was annotated and tracked individually throughout the analysis. For homology conversion, gene symbols from nonmouse species were converted to known mouse homologs based on the Mouse Genome Database—Vertebrate Homology, Mouse Genome Informatics, The Jackson Laboratory, Bar Harbor, Maine.[9]

The data discussed in this publication have been deposited in NCBI's Gene Expression Omnibus[17] and are accessible through GEO Series accession number GSE146215.

2.9. Statistical analysis

Two-tailed Student t-test was used for group differences between Sham and SNI in the von Frey mechanical sensitivity
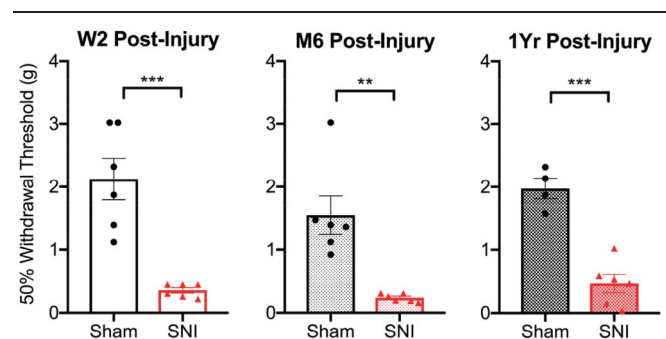
Figure 1. Mechanical hypersensitivity persists for up to 1 year after spared nerve injury (SNI). Nerve-injured mice were hypersensitive to mechanical stimuli compared to sham mice at 2 weeks (W2), 6 months (M6), and 1 year (1Yr) post-SNI. Bars represent mean ± SEM 50% withdrawal threshold expressed in grams. Two-tailed Student t-test, **$P < 0.01$; ***$P < 0.001$, n = 4 to 6/group.

behavioural assay (**Fig. 1**). A two-tailed Welch *t* test was used to test for differences in cell type counts between Sham and SNI (**Fig. 2**). Differences between the magnitude of differential methylation across time points was identified using a Welch analysis of variance (ANOVA) followed by Games–Howell post

hoc test for multiple comparisons (**Fig. 3**). Pairwise comparisons of CpG positions at each time point used a negative binomial generalized linear model to fit the data, and differential methylation was determined using the likelihood ratio test. Analyses were corrected for multiple comparisons using the
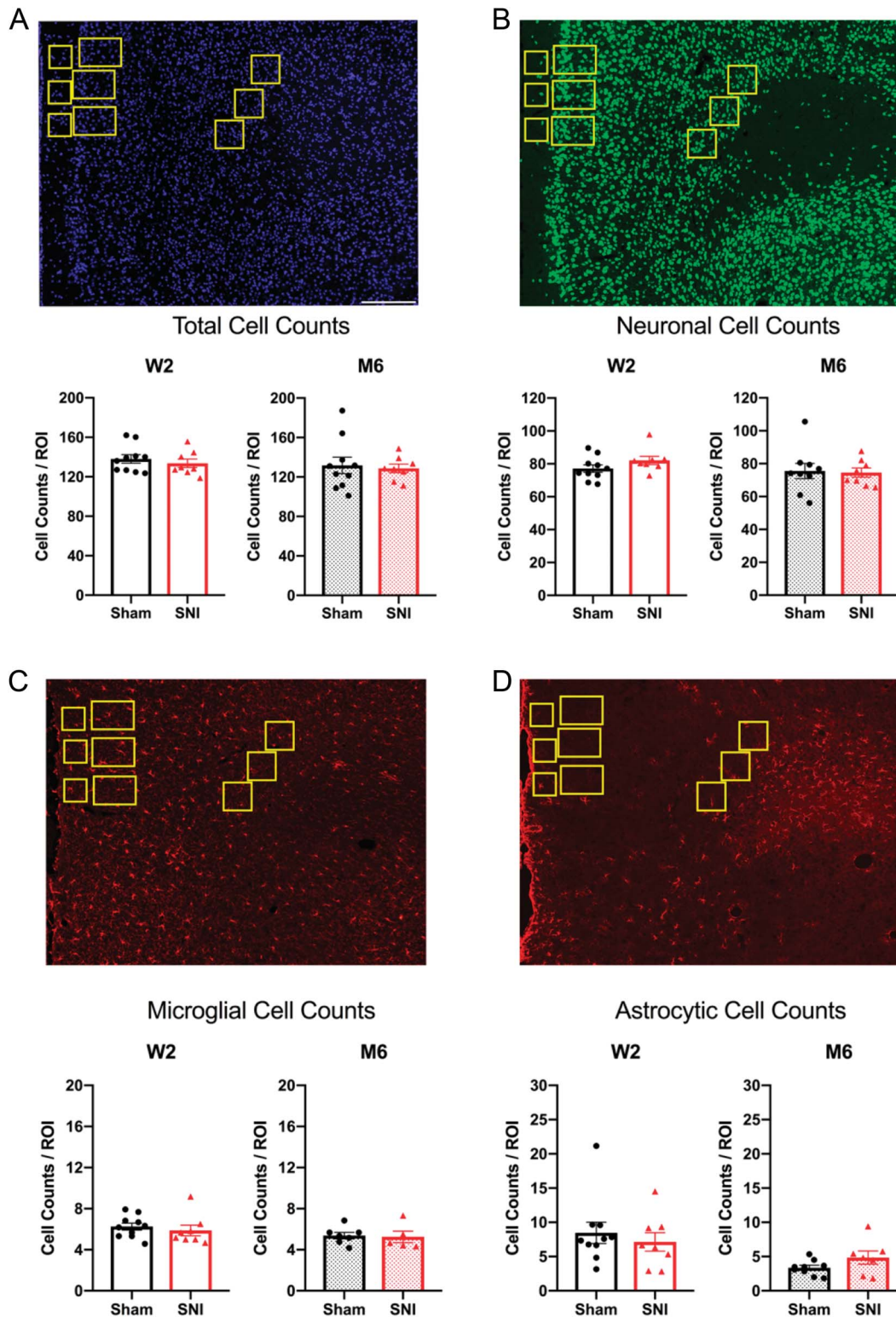
Figure 2. Immunohistochemistry reveals no changes in neuronal, microglial, or astrocytic cell proportions 2 weeks and 6 months after spared nerve injury (SNI). (A) Total (DAPI, Blue), (B) neuronal (NeuN-immunoreactivity (-ir), Green), (C) microglial (Iba1-ir, Red), and (D) astrocytic (GFAP-ir, Red) cell counts in Sham and SNI cortex at W2 or M6 time points. Displayed are average cell counts from all cortical layers from the prelimbic area of the prefrontal cortex. Quantified ROI area is equivalent to 33,040.9 μm^2. Bars represent mean ± SEM cell counts; two-tailed Welch *t* test. No significant differences observed. n = 8 to 10/group. ROI, regions-of-interest.
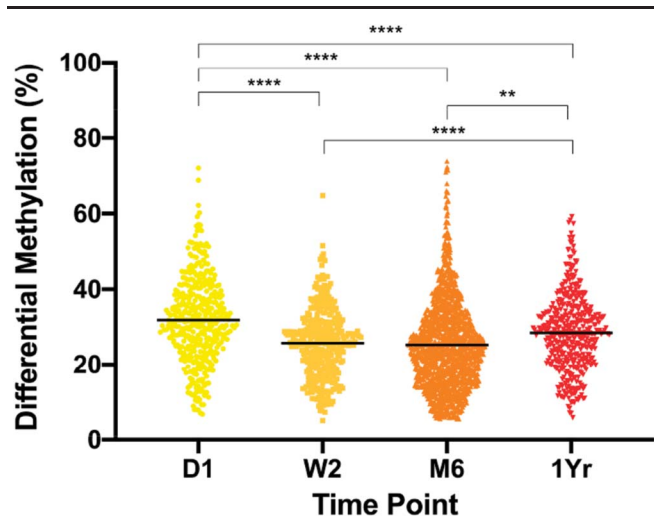
Figure 3. Magnitude of differential methylation after spared nerve injury (SNI). Differential methylation is expressed in terms of absolute percentage of change between Sham and SNI at 1 day (D1), 2 weeks (W2), 6 months (M6), and 1 year (1Yr) postsurgery. Each dot is an individual CpG. Welch ANOVA with Games–Howell test for multiple comparisons. **$P < 0.01$, ****$P < 0.0001$. n = 4 to 8/group. ANOVA, analysis of variance.

Benjamini–Hochberg FDR (**Fig. 4**). Post hoc supervised hierarchical clustering analysis was performed using the Ward method and 1-Pearson correlation as the distance metric (**Figs. 5–8A**). Hypergeometric test was used to test for significant enrichment of pain-related and other experimentally identified genes.

2.10. Gene ontology analysis

Differentially methylated genes identified at each time point were submitted to Metascape,[75] a web-based Gene Ontology tool. The CORUM, the Reactome Gene Sets, the KEGG Pathway, Functional Set and Structural Complex, and the GO Biological Processes, Cellular Component and Molecular Function databases were selected as ontology databases. An ontology was considered enriched at a P-value <0.05, minimum gene count of 3, and a minimum enrichment factor >1.5. At each time point, 15 representative gene ontologies were selected on the basis of P-value, number of DM genes within the ontology, and being a parent term to other identified ontologies. At most, only 66% of DM genes within a representative ontology are identical to the DM genes identified in any other representative ontology.

3. Results

3.1. Spared nerve injury results in long-term neuropathic pain but has no impact on the proportions of neurons, astrocytes, and microglia in the prefrontal cortex

Prior to performing bisulfite sequencing, we validated the presence of long-term neuropathic pain (**Fig. 1**). To control for nonepigenetic mechanisms that might drive differential DNA methylation, we verified that the proportions of neurons, astrocytes, and microglia do not differ between Sham and SNI animals at W2 and M6. Because each cell type has its own DNA methylation profile, differential methylation between Sham and SNI animals could result from the gain or loss of specific cell populations.

3.1.1. Behavioural signs of neuropathic pain persist up to 1 year after spared nerve injury

To confirm long-term neuropathic pain, mechanical sensitivity was assessed using the von Frey assay at 2 weeks, 6 months, and 1 year after SNI. Spared nerve injury animals were more sensitive to mechanical stimuli applied to the plantar surface of the hind paw ipsilateral to the injury at all time points when compared to their respective sham animals (two-tailed Student t-test. W2: $t_{10} = 5.3$, $P = 0.0003$; M6: $t_{10} = 4.2$, $P = 0.002$; 1Yr: $t_8 = 6.8$, $P = 0.0001$) (**Fig. 1**). The reduction in 50% withdrawal thresholds in SNI animals indicates the presence of a persistent and stable mechanical hypersensitivity for up to 1 year.

3.1.2. Spared nerve injury has no impact on the proportions of neurons, astrocytes, and microglia in the prefrontal cortex

The neuronal, astrocytic, and microglial cell populations were quantified in the PFC by immunohistochemistry to quantify SNI-related changes 2 weeks and 6 months after surgery. Overall cell counts were calculated independently in prelimbic and infralimbic cortical areas as well as at 3 cortical depths: layer I, superficial layers (layer II-III), and deep layers (layer V). No significant differences were detected between SNI and Sham for any cell types in either the prelimbic (two-tailed Welch t test. **DAPI** W2: $t_{15.80} = 0.7$, $P = 0.48$; M6: $t_{13.21} = 0.3$, $P = 0.75$. **NeuN** W2: $t_{15.16} = 1.5$, $P = 0.16$; M6: $t_{12.96} = 0.2$, $P = 0.86$. **GFAP** W2: $t_{16} = 0.6$, $P = 0.53$; M6: $t_{7.80} = 1.4$, $P = 0.19$. **Iba1** W2: $t_{12.48} = 0.6$, $P = 0.55$; M6: $t_{6.51} = 0.2$, $P = 0.86$) (**Fig. 2**) or infralimbic (Supplemental Fig. 1, available at http://links.lww.com/PAIN/B27) regions at either time point.

3.2. Spared nerve injury produces rapid, large, and persistent changes in DNA methylation in the prefrontal cortex

Differentially methylated (DM) CpG sites were identified by bisulfite capture sequencing by comparing SNI vs Sham. In this study, only DM CpGs that were annotated to promoter regions were selected for analysis due to the inverse relationship between CpG DNA methylation and gene expression (in general, less methylation = increased gene expression; more methylation = reduced gene expression[68]).

Table 1 shows the number of DM CpG sites after adjusting for multiple comparisons. At each of the 4 time points evaluated, at least 350 DM CpGs were identified at an FDR-adjusted P-value threshold of 0.1. Increasingly stringent thresholds still identify a large number of DM positions. Notably, a subpopulation of DM CpGs remain significant at an FDR-adjusted P-value $< 1 \times 10^{-7}$, representing a substantial and consistent change between Sham and SNI and strong effect of injury.

The magnitude of differential methylation at each time point of all DM CpGs is displayed in **Figure 3**. The average magnitude of differential methylation between Sham and SNI is approximately 25% to 30% at all time points. This is a robust shift in methylation state for most DM CpG positions and is on par with that observed in the brain for major depressive disorder.[31]

The effect of peripheral injury on PFC methylation is immediate, with the largest degree of differential methylation between Sham and SNI detected at D1 postinjury, indicating a rapid response to injury. D1 had a significantly higher average methylation change between Sham and SNI than the other time points (Welch ANOVA followed by Games–Howell post hoc test: D1 vs W2/M6/1Yr, $P < 0.0001$), with 75% of CpGs having a greater than 25% change in methylation, and
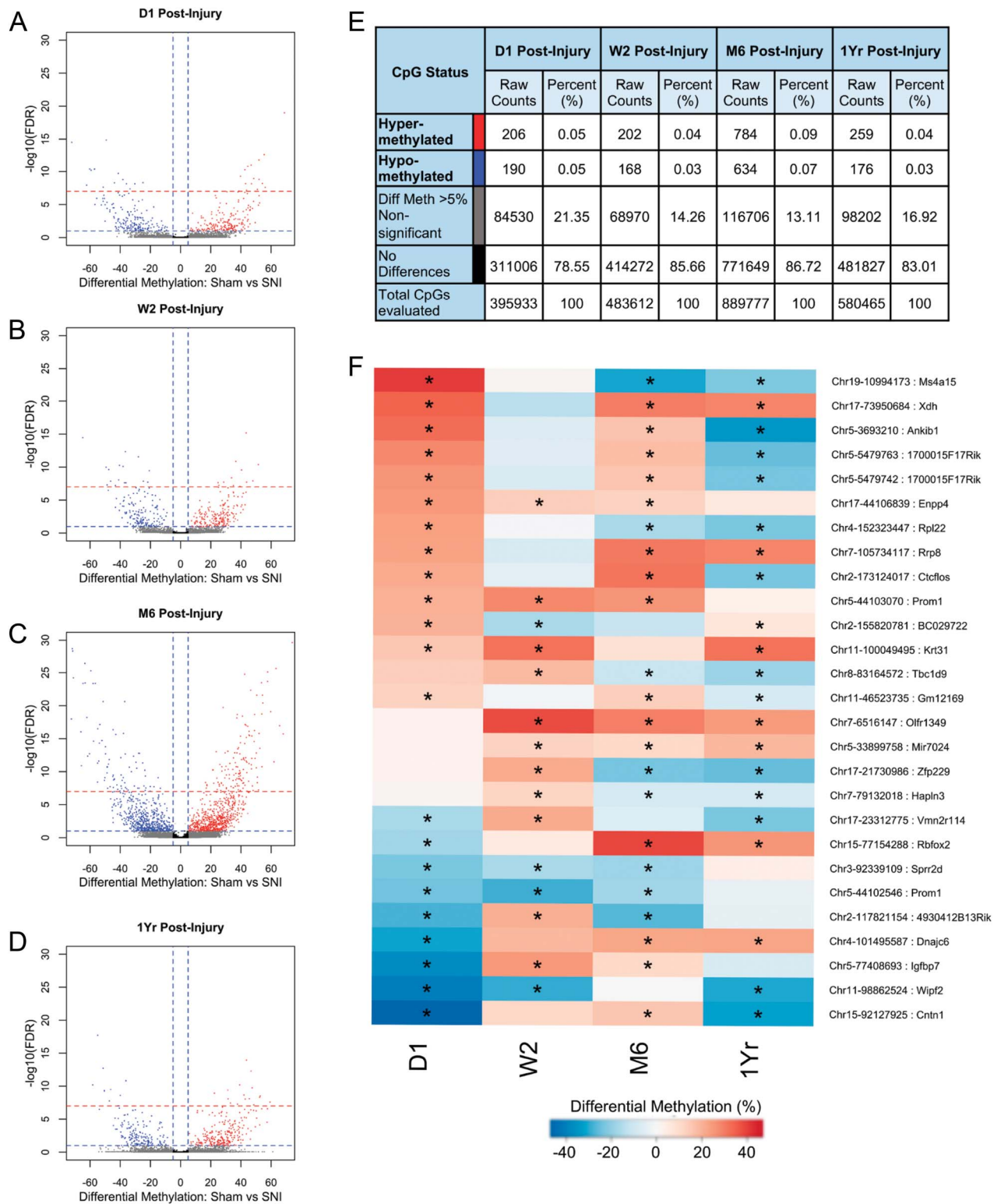
Figure 4. Hypermethylated and hypomethylated CpGs after spared nerve injury (SNI). The magnitude of the statistical significance between methylation differences in promoter region CpGs at (A) 1 day (D1), (B) 2 weeks (W2), (C) 6 months (M6), and (D) 1 year (1Yr) postsurgery. CpGs are displayed in terms of positive or negative methylation difference with Sham as the reference point vs SNI, against −log10 (FDR) on the y-axis. Blue horizontal dashed line indicates an FDR-adjusted P-value threshold of 0.1, and red horizontal dashed line indicates an FDR-adjusted P-value threshold of 1×10^{-7}. The blue vertical dashed line indicates methylation difference thresholds of 5% and −5%. Red dots = hypermethylated CpGs: blue dots = hypomethylated CpGs; gray dots = nonsignificant with methylation differences of >5%, black dots = CpGs that are not different: black. (E) The raw counts and percentage of detected CpGs. (F) Single CpG positions that were significantly different at 3 or more time points were tracked across time and display varying patterns of differential methylation. Values are displayed as differential methylation. *FDR-adjusted P-value <0.1. FDR, false discovery rate.

A

C

D1 Selected Gene Ontologies

B

Gene Name	Average FDR	Average Differential Methylation	# of DM CpGs	Hyper - Hypo
4933421I07Rik	4.26E-03	-32.99	3	0-3
Ahr	9.75E-04	37.45	2	2-0
Banf2	5.77E-10	47.65	2	2-0
BC051537	1.18E-05	-33.49	2	0-2
Ccdc85a	2.29E-05	48.14	2	2-0
Cdc23	3.80E-08	45.41	2	2-0
Cep63	4.05E-03	37.18	3	3-0
Cntn1	6.61E-11	-59.23	1	0-1
Cysltr2	4.79E-04	-53.38	3	0-3
Dcaf11	5.28E-10	39.76	1	1-0
Ddx51	2.55E-03	26.26	3	3-0
Fam109b	1.63E-09	-38.18	1	0-1
H2-Q4	5.03E-03	23.35 / -24.90	2	1-1
Icos	1.92E-05	46	2	2-0
Klk1b24	1.86E-06	-45.84	2	0-2
Mapkbp1	4.16E-11	-60.19	1	0-1
Mid1	3.61E-02	23.58	12	12-0
Mir6993	2.65E-09	52.75	3	3-0
Nacad	4.60E-04	42.72 / -30.28	2	1-1
Olfr1387	5.32E-11	42.67	1	1-0
Olfr316	3.83E-03	-40.88	2	0-2
Sec23b	2.25E-11	-64.6	2	0-2
Smim26	1.02E-19	68.83	1	1-0
Ucp3	1.88E-10	-41.24	1	0-1
Unc5cl	6.11E-06	-46.68	2	0-2

Figure 5. Differentially methylated genes and gene ontologies at 1 day (D1) after spared nerve injury (SNI). (A) Supervis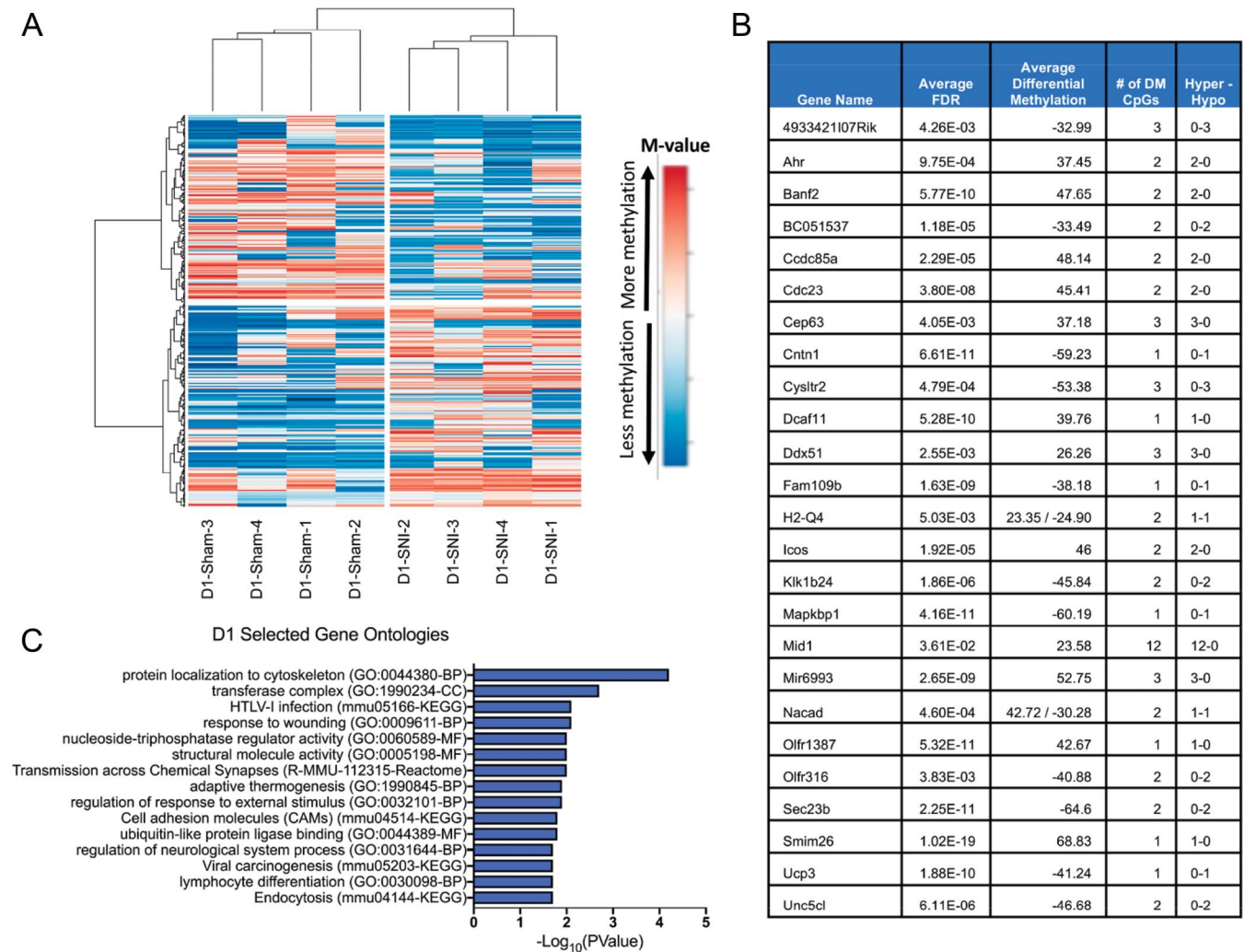ed hierarchical clustering of DM CpGs at each time point displays common patterns of differential methylation between individual animals in the same treatment group. Each column is an individual animal and each row represents a CpG position, with blue being less methylation and red being more methylation. Values are displayed as M-Value: $\log_2$ (# methylated CpGs/# unmethylated CpGs) Clustering method: Ward, distance metric: 1-Pearson correlation. (B) Top 25 differentially methylated genes. (C) Top 15 selected gene ontologies identified. Enriched ontology: minimum gene count of 3, $P < 0.05$, and a minimum enrichment of 1.5. n = 4 mice/group.

25% of CpGs having a change larger than 38%. The W2 and 1Yr time points were the most tightly clustered, with 50% of DM CpGs within 6% to 7% of their mean differential methylation. Despite having the lowest average percent differential methylation, the M6 time point had a large subpopulation skewed towards high levels of methylation change. These highly DM CpGs may play an important role in the transition from subacute to chronic pain.

The effect of injury upon PFC methylation is also persistent, with differential methylation observed throughout the time course. Within each time point, there were no significant differences in the number of hypermethylated vs hypomethylated CpGs. (**Figs. 4A–E**). This balance suggests locus-specific methylation targeting as opposed to a global increase or decrease in DNA methylation.

To explore how patterns of methylation evolve at individual CpGs across time, we grouped all CpGs that were DM at a minimum of 3 of the 4 time points (**Fig. 4F**). Although the direction of differential methylation is largely consistent across time for some CpGs, others display dynamic patterns as a function of chronicity. For example, the actin cytoskeleton remodeling gene, WAS/WASL interacting protein family member 2 (*Wipf2*), is consistently hypomethylated, whereas the cell adhesion gene Contactin 1 (*Cntn1*) fluctuates between hypomethylation and hypermethylation across the entire

time course. Taken together, the DNA methylation response to peripheral nerve injury is rapid, large, and dynamic, and persists throughout the entire time course.

3.3. Spared nerve injury results in time point-specific differential methylation of individual genes and functional pathways in the prefrontal cortex

To determine the functional impact of these substantial shifts in the PFC methylation landscape, we performed gene annotation and downstream analyses to identify associated genes and gene ontologies.

Differentially methylated CpGs were annotated to their corresponding gene based on the mm10 reference genome. We found that 61.3% of annotated CpGs were the only DM CpG annotated to a gene promoter within a time point. By contrast, 35.5% of annotated CpGs were part of clusters of 2 to 6 DM CpGs annotated to a promoter region and the remaining 3.3% of CpGs existed within clusters of 7+ CpGs, corresponding to the promoters of 4 genes: *Organic Solute Carrier Partner 1 (Oscp1), Midline1 (Mid1), Toll-like receptor 6 (Tlr6), and 1110020A21Rik.*

Table 1

Spared nerve injury (SNI) results in highly significant differentially methylated (DM) CpG positions in prefrontal cortex.

FDR	D1	W2	M6	1Yr
1.0×10^{-7}	31	28	214	25
1.0×10^{-6}	43	42	259	41
1.0×10^{-5}	62	58	344	62
1.0×10^{-4}	87	91	424	100
0.001	120	141	605	156
0.01	205	232	883	257
0.1	**396**	**370**	**1418**	**435**
0.2	508	487	1767	541

SNI induces DM CpGs at all time points. Bolded figures indicate DM CpGs at FDR-adjusted P-value experimental threshold of 0.1. Likelihood ratio test with Benjamini–Hochberg false discovery rate correction for multiple comparisons.
FDR, false discovery rate.

Of the genes identified with multiple DM CpGs within a time point, the majority (88.5%) were either all hypermethylated or all hypomethylated within that promoter, suggesting that the resulting dysregulated genes are likely to be either upregulated or downregulated.

Supervised clustering was performed at each time point to visualize clusters of covarying DM CpGs and the characteristic methylation profile of Sham and SNI animals (**Figs. 5A–8A**).

To identify the most DM genes at each time point, a promoter region index was determined by multiplying the adjusted P-value of each CpG by the number of CpGs within the promoter region. The top 25 DM genes at each time point as determined by promoter region index can be viewed in **Figures 5B–8B**, listing the average adjusted P-value, average differential methylation, number of DM CpGs identified within the gene promoter, and number of hypermethylated or hypomethylated DM CpGs. In cases with mixed differential methylation in the promoter, the average methylation for both hypermethylated and hypomethylated CpGs are shown separately. Full lists displaying individual DM CpGs and their annotated genes are available in Supplemental Table 3 (available at http://links.lww.com/PAIN/B23).

To identify broader effects of differential gene methylation and therefore potential functional dysregulation, gene ontologies enriched for DM genes were also identified (**Figs. 5C–8C**). The full list of enriched ontologies by time point can be observed in Supplemental Table 4 (available at http://links.lww.com/PAIN/B24).

3.3.1. One day postinjury

At D1, 396 DM CpGs identified 327 unique genes undergoing differential methylation in their promoter region. The top 25 DM genes were related to cell–cell interaction (*Ccdc85a, Cntn1*), cell structure (*Banf2, Cep63, Mid1*), and immune response (*Cystlr2, H2-Q4, Icos, Mapkbp1, Unc5cl*) (**Fig. 5B**). *Mapkbp1, H2-Q4, Icos*, and *Unc5cl* have involvement in TLR, NFκB, and TNF signaling pathways, with additional immune-related genes *Acod1, Cd14, Itch, H2-K1, H2-M1, Mapkapk3, Mapkapk5*, and *Tnfrsf13c* also identified as DM at this time point. Although not part of the top 25 DM genes, actin and cytoskeletal dynamics genes (*Acta2, Diaph1, Dvl1, Macf1, Wipf2*) are also observed.

Gene ontology analysis identified functional pathways enriched for DM genes involved in response to stimulus, cellular structure remodeling, and extracellular matrix formation (**Fig. 5C**).

3.3.2. Two weeks postinjury

At W2, 370 DM CpGs identified 311 unique genes undergoing differential methylation in their promoter region. The top 25 DM genes had involvement in actin processes (*Mical3*), cell surface molecules (*Gpc6, Prom1*), and immune regulation (*Btla, Ccl7*) (**Fig. 6B**). In addition to the top 25, the W2 time point revealed genes involved in cellular structure and organization processes, such as actin and cytoskeleton (*Capza3, Epb41l1, Fhdc1, Myh2, Mprip, Shroom3, Tns1, Tns4, Wipf2*), extracellular matrix (*Col4a1, Col6a4, Halpn3, Rpsa*), and cell–cell interactions (*Nectin2, Lgals4*). Also of interest is the differential methylation of *Ramp1*, which is crucial for the maturation and transport of CALCRL and its function as the CGRP receptor.

At W2, identified gene ontologies are involved with cellular structure remodeling, extracellular matrix, response to stimulus, and changes to internal cellular functioning (**Fig. 6C**).

3.3.3. Six months postinjury

At M6, 1418 DM CpGs identified 1001 unique genes undergoing differential methylation in their promoter region. The top 25 DM genes were involved in E3 ubiquitination (*Mid1, Trim21, Trim30d*) and immune functioning (*Gdf15, Fam129c, Arhgef2*) (**Fig. 7B**). In addition to the top 25, the M6 time point also displays a substantial number of immune genes across many different pathways (*Cd6, Ltbp1, Trem2;* TNF: *Traf3ip1, Traf6;* Interleukin: *Il12b, Il12rb1, Jak3;* TLR: *Lbp, Acod1, Myd88, Tlr6*). Actin regulation and formation is also affected, with numerous DM GTPases and guanine exchange factors (*Arhgap8, Arhgap15, Arhgap17, Arhgap33os, Arhgef2, Arhgef10l, Arhgef17, Arhgef19*).

At M6, the gene ontologies are related to immunological responses and systems, transcription factors, signaling cascades, and enzymatic processes (**Fig. 7C**).

3.3.4. One year postinjury

At 1Yr, 435 DM CpGs identified 359 unique genes undergoing differential methylation in their promoter region. The top 25 DM genes are involved in actin regulation (*Mprip, Parva, Txnrd1*), histone methylation (*Smyd1*), and the acid-sensing channel *Asic3* (**Fig. 8B**), In addition to the top 25, genes were identified that are involved with cell adhesion molecules (*Cldn13, Cldn15, Hapln3, Madcam1, Nectin2, Nfasc*) and extracellular matrix (*Col17a1, Lama3*).

At 1Yr, the top selected gene ontologies are related to cellular signaling, extracellular matrix formation, and cellular function regulation (**Fig. 8C**).

3.4. Spared nerve injury results in function-specific responses across the time course

To identify trends in the functional responses to peripheral nerve injury across time, we overlapped all gene ontologies that were significantly enriched in DM genes at all time points. Overall, of the 775 enriched gene ontologies identified across all 4 time points, 658 gene ontologies were unique to one time point, 91 overlapped across 2 time points, 6 were found at 3 time points, and none were found to overlap across all 4 time points (**Fig. 9A**). Displayed are the top 5 overlapping ontologies between time points, as determined by greatest averaged P-values and a minimum of 3 enriched genes at each time point in the ontology (**Fig. 9B**). When identifying the overlapping gene ontologies at

A

C

W2 Selected Gene Ontologies

B

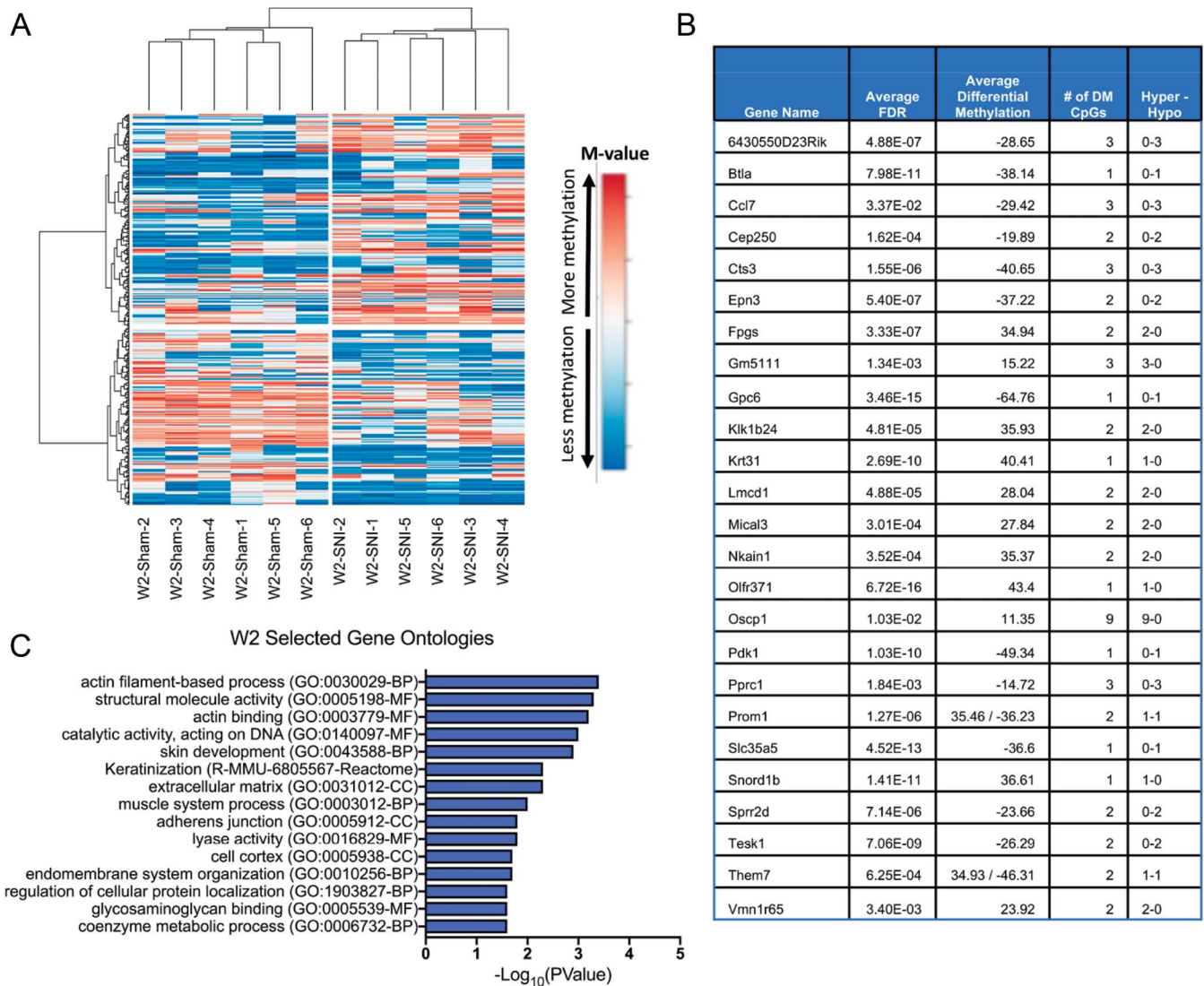| Gene Name	Average FDR	Average Differential Methylation	# of DM CpGs	Hyper - Hypo
6430550D23Rik	4.88E-07	-28.65	3	0-3
Btla	7.98E-11	-38.14	1	0-1
Ccl7	3.37E-02	-29.42	3	0-3
Cep250	1.62E-04	-19.89	2	0-2
Cts3	1.55E-06	-40.65	3	0-3
Epn3	5.40E-07	-37.22	2	0-2
Fpgs	3.33E-07	34.94	2	2-0
Gm5111	1.34E-03	15.22	3	3-0
Gpc6	3.46E-15	-64.76	1	0-1
Klk1b24	4.81E-05	35.93	2	2-0
Krt31	2.69E-10	40.41	1	1-0
Lmcd1	4.88E-05	28.04	2	2-0
Mical3	3.01E-04	27.84	2	2-0
Nkain1	3.52E-04	35.37	2	2-0
Olfr371	6.72E-16	43.4	1	1-0
Oscp1	1.03E-02	11.35	9	9-0
Pdk1	1.03E-10	-49.34	1	0-1
Pprc1	1.84E-03	-14.72	3	0-3
Prom1	1.27E-06	35.46 / -36.23	2	1-1
Slc35a5	4.52E-13	-36.6	1	0-1
Snord1b	1.41E-11	36.61	1	1-0
Sprr2d	7.14E-06	-23.66	2	0-2
Tesk1	7.06E-09	-26.29	2	0-2
Them7	6.25E-04	34.93 / -46.31	2	1-1
Vmn1r65	3.40E-03	23.92	2	2-0

Figure 6. Differentially methylated genes and gene ontologies 2 weeks (W2) after spared nerve injury (SNI). (A) Supervised hierarchical clustering of DM CpGs at each time point displays common patterns of differential methylation between individual animals in the same treatment group. Each column is an individual animal and each row represents a CpG position, with blue being less methylation and red being more methylation. Values are displayed as M-Value: $\log_2$ (# methylated CpGs/# unmethylated CpGs) Clustering method: Ward, distance metric: 1-Pearson correlation. (B) Top 25 differentially methylated genes. (C) Top 15 selected gene ontologies identified. Enriched ontology: minimum gene count of 3, $P < 0.05$, and a minimum enrichment of 1.5. n = 6 mice/group. DM, differentially methylated.

each time point, early time points D1 and W2 display ontologies more related to responding to external stimuli and damage, whereas later time points M6 and 1Yr display ontologies more related to adaptive immune response and T-cell-mediated cytotoxicity. In all overlapping ontologies between time points, there is a strong contribution of actin and cytoskeleton-related ontologies. These dysregulated pathways may contribute to the functional and structural cortical remodeling previously reported in chronic pain conditions.

3.5. Pain-related genes show time point-specific patterns of differential methylation

To determine whether any of the identified DM genes had been previously linked to pain, we cross-referenced with data sets of previously identified pain-related genes (**Fig. 10**). Ultsch et al.[66] previously identified 535 human and mouse genes associated with pain. After conversion to mouse gene homologs, we identified 31 DM pain-related genes representing a significant enrichment (hypergeometric test, $P = 0.03$). The Human Pain Genes Database (HPGD) has identified 361 genes in humans wherein SNPs have been found to affect the sensation of pain.[47] Two hundred eighty-nine HPGD genes had known mouse homologs, of which 15 DM genes were found in our data set, but was not significantly enriched (hypergeometric test, $P = 0.21$).

When tracking the differential methylation pattern of pain-related genes across the time course, most only show differential methylation at one time point. At D1, pain-related genes were involved in immune response (*Cd14*), and a number of ion channels (*Chrnb4, Gabrr1, Kcnk18*). At W2, pain-related genes were related to actin (*Ablim3*), immune regulation (*Ccl2, Ccl7*), and ion channels (*Cacna1g, Kcnk5, Scn10a*). At M6, identified pain-related genes are involved in immune responses (*Ccl2, Ccl7, Dpp4, Myd88, Pik3cg, Tnf*), cell-cycle regulation (*Taok3*), and ion channels and transport

A

B

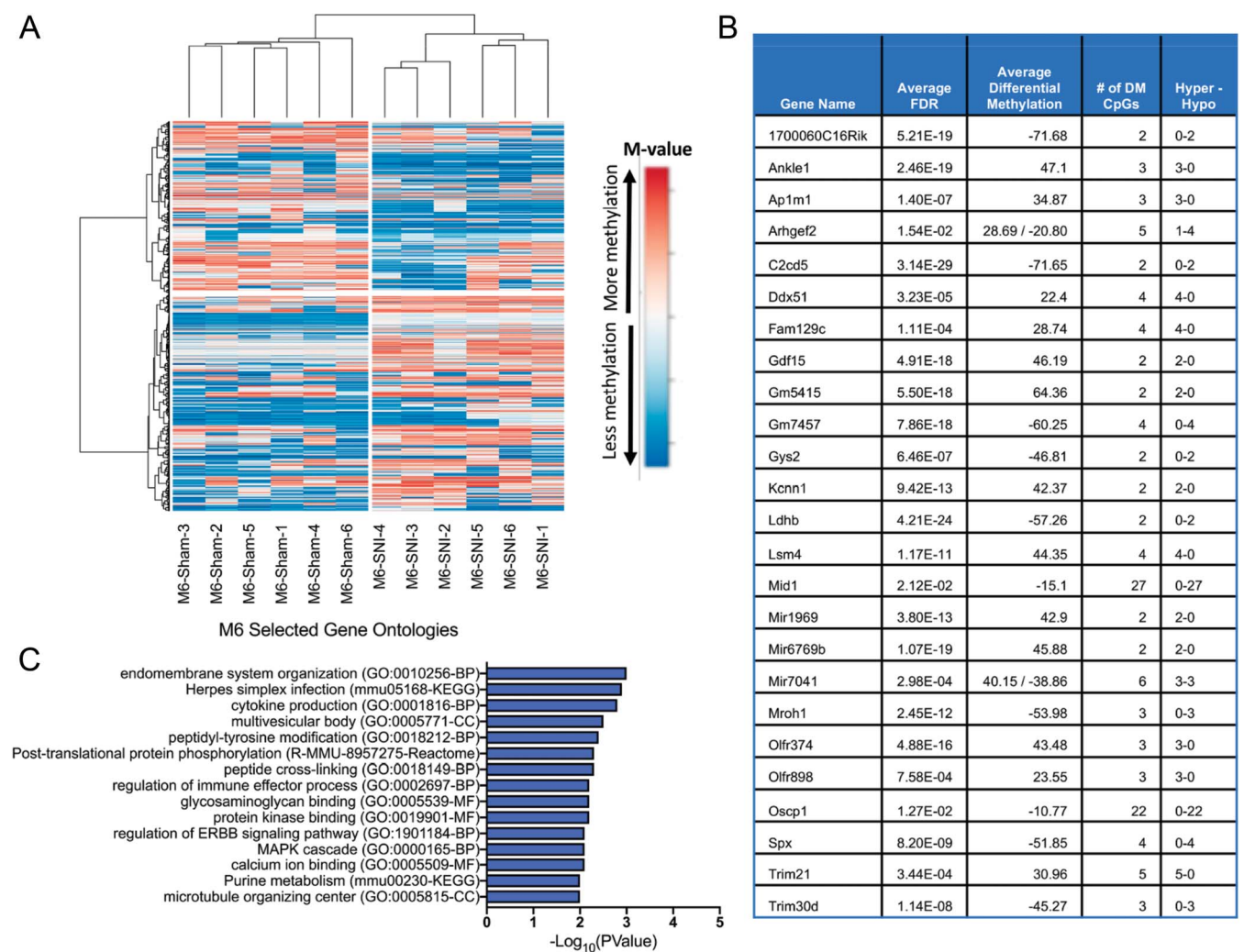| Gene Name	Average FDR	Average Differential Methylation	# of DM CpGs	Hyper - Hypo
1700060C16Rik	5.21E-19	-71.68	2	0-2
Ankle1	2.46E-19	47.1	3	3-0
Ap1m1	1.40E-07	34.87	3	3-0
Arhgef2	1.54E-02	28.69 / -20.80	5	1-4
C2cd5	3.14E-29	-71.65	2	0-2
Ddx51	3.23E-05	22.4	4	4-0
Fam129c	1.11E-04	28.74	4	4-0
Gdf15	4.91E-18	46.19	2	2-0
Gm5415	5.50E-18	64.36	2	2-0
Gm7457	7.86E-18	-60.25	4	0-4
Gys2	6.46E-07	-46.81	2	0-2
Kcnn1	9.42E-13	42.37	2	2-0
Ldhb	4.21E-24	-57.26	2	0-2
Lsm4	1.17E-11	44.35	4	4-0
Mid1	2.12E-02	-15.1	27	0-27
Mir1969	3.80E-13	42.9	2	2-0
Mir6769b	1.07E-19	45.88	2	2-0
Mir7041	2.98E-04	40.15 / -38.86	6	3-3
Mroh1	2.45E-12	-53.98	3	0-3
Olfr374	4.88E-16	43.48	3	3-0
Olfr898	7.58E-04	23.55	3	3-0
Oscp1	1.27E-02	-10.77	22	0-22
Spx	8.20E-09	-51.85	4	0-4
Trim21	3.44E-04	30.96	5	5-0
Trim30d	1.14E-08	-45.27	3	0-3

C

Figure 7. Differentially methylated genes and gene ontologies 6 months (M6) after spared nerve injury (SNI). (A) Supervised hierarchical clustering of DM CpGs at each time point displays common patterns of differential methylation between individual animals in the same treatment group. Each column is an individual animal and each row represents a CpG position, with blue being less methylation and red being more methylation. Values are displayed as M-Value: $\log_2$ (# methylated CpGs/# unmethylated CpGs) Clustering method: Ward, distance metric: 1-Pearson correlation. (B) Top 25 differentially methylated genes. (C) Top 15 selected gene ontologies identified. Enriched ontology: minimum gene count of 3, $P < 0.05$, and a minimum enrichment of 1.5. n = 6 mice/group.

(*Chrm3, Kcnk5, Scn2b, Scn10a, Slc24a3*). At 1Yr, pain-related genes were involved in ion channels (*Asic3, Kcnj9, Trpv1*), peptide signaling (*Tac4*), and G-protein-coupled receptor signaling (*P2ry12*).

For pain-related CpGs that were able to be captured at all time points, only 3 CpGs had differential methylation at more than one time point (*P2ry12, Gal,* and *Ccl2*) (**Fig. 10A**). Interestingly, galanin (*Gal*) and chemokine ligand 2 (*Ccl2*) both show reversals of their methylation state from W2 to M6. The methylation reversal of these 2 pain genes may indicate that the recruitment of pain-related processes may change across the time course, and genes have a temporal impact upon chronic pain development. Although limited by a lack of data at all time points, a similar time point-specific pattern of significant differential methylation was observed for CpGs that were not captured at all time points (**Fig. 10B**). Therefore, although a gene may be pain-related, its contribution to a pain phenotype may be restricted or limited in time.

We also cross-referenced our M6 experimental genes with 2 gene sets identified in our previous studies. Massart et al. 2016 examined rat PFC DNA methylation at 9 months post-SNI and identified 3981 genes that undergo differential methylation, with 3011 identified

mouse homologs.[43] Our data set was significantly enriched for genes identified by Massart et al. (hypergeometric test, $P = 0.02$), with 107 overlapping genes and 56 genes with consistent differential methylation profiles between the 2 species (Supplemental Table 5, available at http://links.lww.com/PAIN/B25). Alvarado et al. 2013 examined mouse PFC mRNA expression using RNAseq at 6 to 8 months post-SNI and identified 641 differentially expressed genes.[1] Our data set was again enriched for genes identified by Alvarado et al. (hypergeometric test, $P = 8 \times 10^{-4}$), with 27 overlapping genes and 12 DM genes consistent with the predicted change in mRNA expression (Supplemental Table 6, available at http://links.lww.com/PAIN/B26).

The NMDA receptor subunit *Grin1* was identified in all 3 data sets, showing both consistent methylation across species and the predicted impact on mRNA expression. Gene regulatory gene *Eif3g* and neurite outgrowth inhibitor *Rtn4* were among the genes consistent between M6 genes and Massart et al. Among the gene consistent between M6 and Alvarado et al. were the cell–cell junction desmosome gene *Dsg1c*, the actin regulatory gene *Cobl*, and the calcium/calmodulin-dependent protein kinase *Camk1d*.
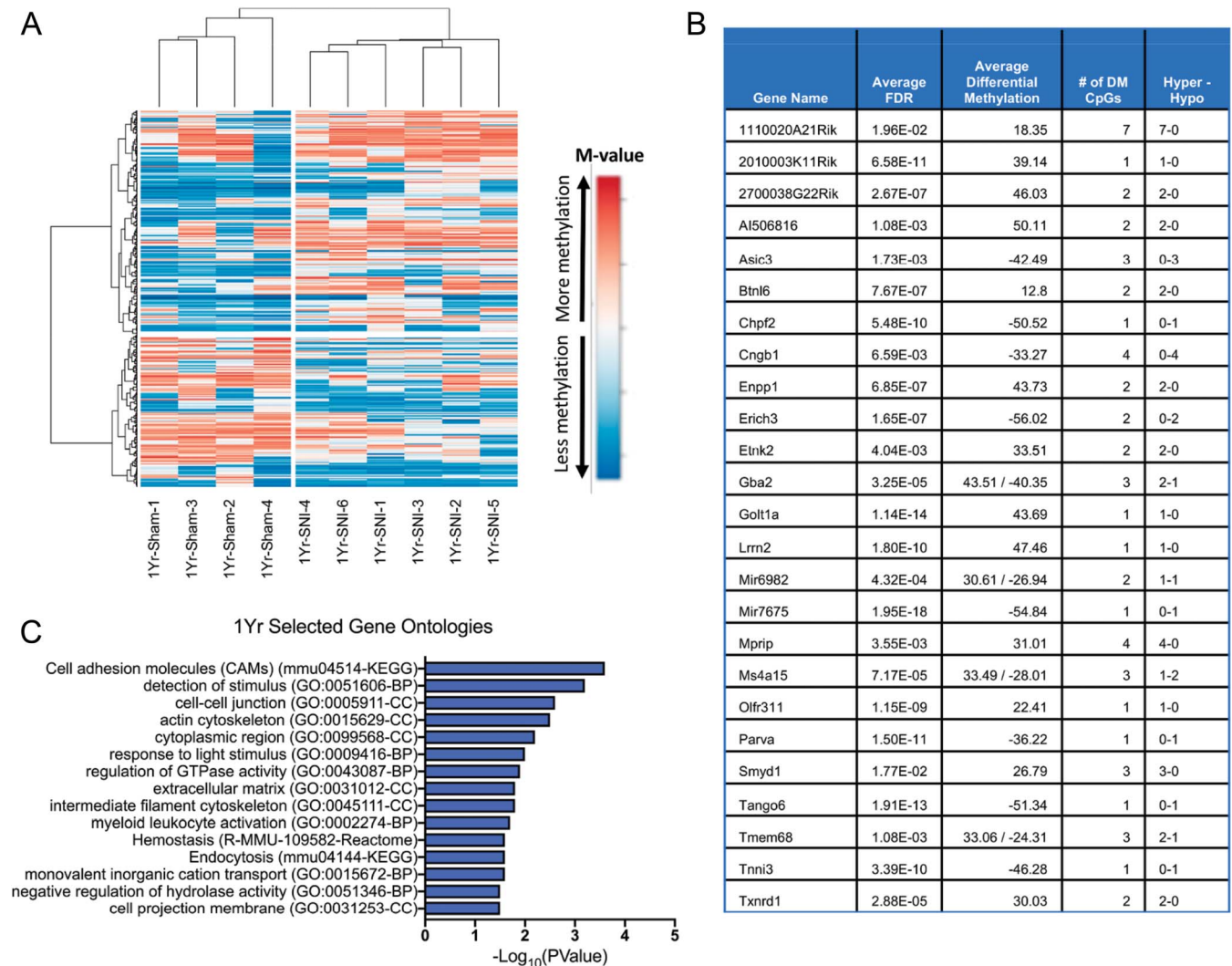
A

M-value

More methylation

Less methylation

1Yr-Sham-1
1Yr-Sham-3
1Yr-Sham-2
1Yr-Sham-4
1Yr-SNI-4
1Yr-SNI-6
1Yr-SNI-1
1Yr-SNI-3
1Yr-SNI-2
1Yr-SNI-5

B

Gene Name	Average FDR	Average Differential Methylation	# of DM CpGs	Hyper - Hypo
1110020A21Rik	1.96E-02	18.35	7	7-0
2010003K11Rik	6.58E-11	39.14	1	1-0
2700038G22Rik	2.67E-07	46.03	2	2-0
AI506816	1.08E-03	50.11	2	2-0
Asic3	1.73E-03	-42.49	3	0-3
Btnl6	7.67E-07	12.8	2	2-0
Chpf2	5.48E-10	-50.52	1	0-1
Cngb1	6.59E-03	-33.27	4	0-4
Enpp1	6.85E-07	43.73	2	2-0
Erich3	1.65E-07	-56.02	2	0-2
Etnk2	4.04E-03	33.51	2	2-0
Gba2	3.25E-05	43.51 / -40.35	3	2-1
Golt1a	1.14E-14	43.69	1	1-0
Lrrn2	1.80E-10	47.46	1	1-0
Mir6982	4.32E-04	30.61 / -26.94	2	1-1
Mir7675	1.95E-18	-54.84	1	0-1
Mprip	3.55E-03	31.01	4	4-0
Ms4a15	7.17E-05	33.49 / -28.01	3	1-2
Olfr311	1.15E-09	22.41	1	1-0
Parva	1.50E-11	-36.22	1	0-1
Smyd1	1.77E-02	26.79	3	3-0
Tango6	1.91E-13	-51.34	1	0-1
Tmem68	1.08E-03	33.06 / -24.31	3	2-1
Tnni3	3.39E-10	-46.28	1	0-1
Txnrd1	2.88E-05	30.03	2	2-0

C

1Yr Selected Gene Ontologies

Cell adhesion molecules (CAMs) (mmu04514-KEGG)
detection of stimulus (GO:0051606-BP)
cell-cell junction (GO:0005911-CC)
actin cytoskeleton (GO:0015629-CC)
cytoplasmic region (GO:0099568-CC)
response to light stimulus (GO:0009416-BP)
regulation of GTPase activity (GO:0043087-BP)
extracellular matrix (GO:0031012-CC)
intermediate filament cytoskeleton (GO:0045111-CC)
myeloid leukocyte activation (GO:0002274-BP)
Hemostasis (R-MMU-109582-Reactome)
Endocytosis (mmu04144-KEGG)
monovalent inorganic cation transport (GO:0015672-BP)
negative regulation of hydrolase activity (GO:0051346-BP)
cell projection membrane (GO:0031253-CC)

$-Log_{10}(PValue)$

Figure 8. Differentially methylated genes and gene ontologies 1 year (1Yr) after spared nerve injury (SNI). (A) Supervised hierarchical clustering of DM CpGs at each time point displays common patterns of differential methylation between individual animals in the same treatment group. Each column is an individual animal and each row represents a CpG position, with blue being less methylation and red being more methylation. Values are displayed as M-Value: log_2 (# methylated CpGs/ # unmethylated CpGs) Clustering method: Ward, distance metric: 1-Pearson correlation. (B) Top 25 differentially methylated genes. (C) Top 15 selected gene ontologies identified. Enriched ontology: minimum gene count of 3, $P < 0.05$, and a minimum enrichment of 1.5. n = 4 to 6 mice/group. DM, differentially methylated.

4. Discussion

This study evaluated DNA methylation as a mechanism for the long-term embedding of injury-related pain in PFC and subsequent evolution of chronic pain. Previous studies have demonstrated DNA methylation responses to chronic pain in rodent PFC[43,63]; however, a number of questions still remain. Are changes in DNA methylation a consequence of chronic pain or do changes precede its emergence? How rapidly do DNA methylation changes occur, and are they persistent throughout chronic pain's time course? Are these changes limited to pain genes, or do they affect entire domains and gene families? What can these changes tell us about how chronic pain develops and embeds itself? Finally, and most importantly, which of these processes should be targeted for intervention?

To answer these questions, we tracked PFC DNA methylation profiles for 1 year post-SNI. We provide first evidence that the PFC methylome is reprogrammed immediately after injury at D1. These data, together with results showing rapid DNA methylation changes in dorsal horn and DRG after injury,[20,40] suggest that changes in DNA methylation precede the emergence of chronic pain. Second, we show that SNI triggers a cascade of dynamic and evolving DNA methylation changes that continue up to 1 year postinjury, suggesting that DNA methylation changes accompany the onset and establishment of chronic pain phenotypes. Third, we identified hundreds of DM genes and gene ontologies. Although some may be relevant at only one time point, DM genes throughout the time course could embed a genomic memory of the initial injury necessary for chronic pain development.

4.1. CpG methylation dynamics

We first analyzed differential CpG methylation between Sham and SNI at each time point independently. At one day postinjury, we observed differential methylation of hundreds of specific CpG positions in the PFC. The D1 time point had the largest average differential methylation, illustrating that the response of the PFC methylome to injury is rapid and substantial. Each time point had
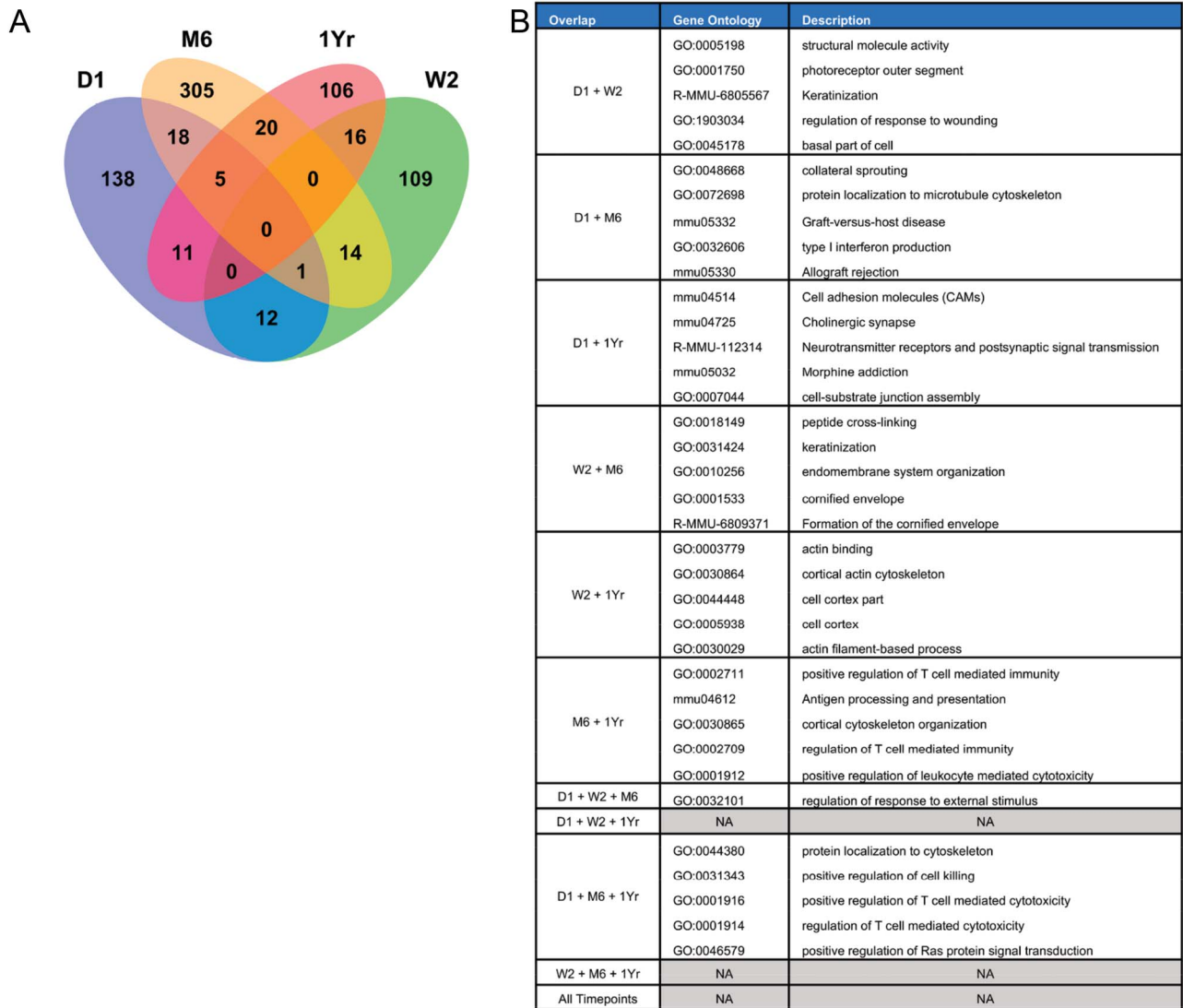
Figure 9. Overlap of dysregulated gene ontologies across time after spared nerve injury (SNI). (A) Gene ontology analysis reveal that 658 of 775 identified enriched ontologies are unique to one time point, with only 91 ontologies overlapping at 2 or more time points. (B) The top 5 gene ontologies per overlap as determined by greatest averaged *P*-value and a minimum of 3 enriched genes at each time point in the ontology.

DM CpGs that displayed a substantial significant difference (FDR adjusted *P*-value <1E-7) and large changes in differential methylation (>40%), indicating that strong methylation changes take place throughout the chronic pain time course.

The presence of both hypermethylated and hypomethylated CpG positions at each time point implies targeted regulation rather than genome-wide increases or decreases in methylation. We previously observed that global DNA methylation decreases after SNI[63]; however, this difference may be due to nonspecific demethylation of nonpromoter regions in the genome.

4.2. Differentially methylated genes, pathways, and functions

We identified 1633 total unique genes that experience differential promoter methylation, of which 31 and 15 genes were members of the pain-related gene lists by Ultsch et al. or HPGD, respectively. Thus, chronic pain affects not just a few candidate genes but also functionally related groups of genes. Each time point had at least 300 DM genes identified, and over 150 enriched gene ontologies. At the early time points of D1 and W2, we observed a greater number of ontologies involved in the response to external stimuli, whereas at the

later time points of M6 and 1Yr, inflammatory and T-cell adaptive immune responses are implicated. Interestingly, across all 4 time points, numerous ontologies involved in actin dynamics or cytoskeletal regulation were identified. Actin reorganization has been previously identified as a key step in inflammation-related persistent pain in glial cells in the spinal cord,[24] and sensory neurons in the periphery.[16] The reorganization of nociceptive circuits and dendritic pruning in response to peripheral neuropathic pain is well established,[48,64,65] and may be a form of maladaptive synaptic plasticity. The consistent differential methylation of actin and cytoskeleton-related genes throughout the time course up to 1 year postinjury suggests an ongoing cortical plasticity and remodeling in response to peripheral injury, and that chronic pain induces progressively greater deviations from normal cortical functioning.

A number of DM genes were consistent with previous results. The NMDA receptor subunit *Grin1* was hypomethylated in both mouse and rat PFC 6 and 9 months post-SNI, respectively, with corresponding increases in Grin1 mRNA expression in mouse cortex during the same time frame.[1,43] Other studies have demonstrated that postinjury changes in PFC in NMDA receptor currents, and modulation of PFC NMDA activity can result in pain
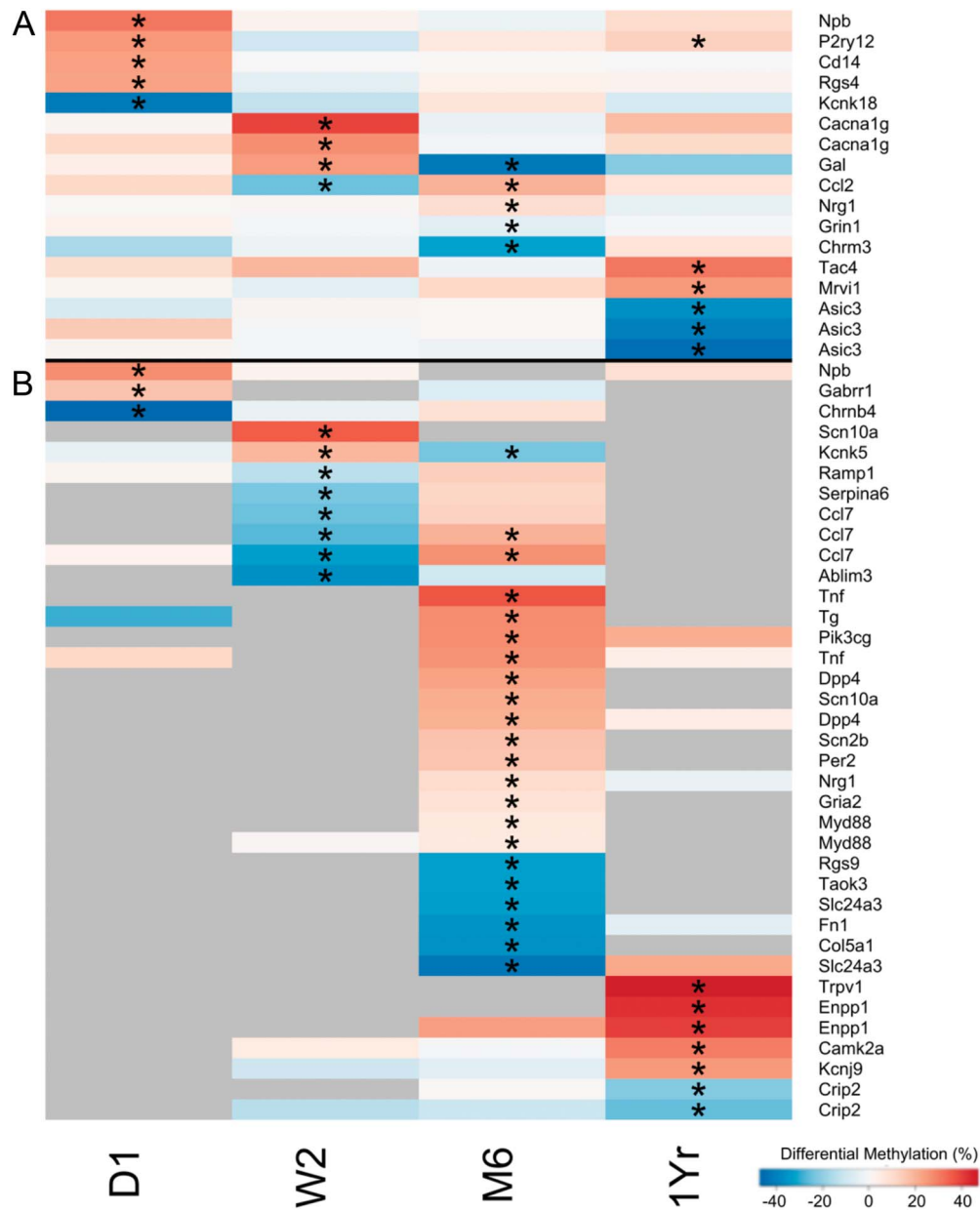
Figure 10. Identification and time course of differentially methylated CpGs associated with pain-related genes. Displayed are CpG positions that were annotated to a pain-related gene identified by Ultsch et al.[66] or the Human Pain Genes Database (HPGD).[47] (A) For CpGs that were captured at all time points, pain-related genes show mostly single time point differential methylation. (B) For CpG positions that were not captured at all time points, there is a trend towards single time point differential methylation. Values are displayed as differential methylation. *FDR adjusted P-value < 0.1. Gray = no data for that gene/time point. FDR, false discovery rate.

modulation.[48,50] Hypomethylation of Grin1 may drive pain-related neuroplasticity, and suggests that NMDA-dependent synaptic changes in chronic pain may be epigenetically mediated. Other genes including *Camk1d, Kcnip2,* and *Cobl* were also consistent between differential methylation and mRNA expression. These converging lines of evidence across different studies highlight potentially pivotal pain-related genes.

4.3. Time point-specific methylation patterns across the chronic pain time course

Differentially methylated CpGs follow distinctive trajectories of differential methylation across the progression from acute to

chronic pain. These differential methylation profiles are a time stamp for the contributions of each gene during chronic pain development and shed light on the postinjury response. Genes with DM CpGs that maintain a methylated state throughout the time course, such as *Wipf2, Rrp8, Xdh, or Sprr2d*, may encode a persistent genomic memory of the initial injury, triggering and maintaining a chronic pain state.

It is important to also consider the time point-specific differential methylation of genes. Nearly all identified pain-related genes were DM at a single time point, implying a time-dependent recruitment or dysregulation of normal functioning. *Grin1, Nrg1, Asic3, Gabrr1, Scn10a, Ramp1, Myd88, Trpv1, and Tnf* had differential methylation at only one observed time point.

All impact pain sensation across domains of ion channel activity and trafficking, inflammatory responses, and neurotransmitter regulation.[15,18,25–27,30,38,39,41,42,44,45,62,67,74]

The time point-specific gene differential methylation and ontology enrichment underscore the importance of understanding temporal dynamics and effects upon normal functioning during the transition to chronic pain. Here, we describe the methylation response of the PFC across all phases of the pain phenotype. At one day postinjury, differential PFC methylation is likely driven by tonic sensory afferent signalling and systemic effects of peripheral inflammation, consistent with enrichment in genes related to response to external stimuli. As pain becomes more chronic by 2 weeks postinjury, central mechanisms including central sensitization and neuroinflammation initiate changes in synaptic signalling and neuron–glia interactions in PFC. By 6 months and 1 year postinjury in late-stage chronic pain, genes involved in immune function become enriched. Late-stage chronic pain is further characterized by dysregulation of descending inhibitory and facilitatory pain pathways, long-term neuroinflammation, neuroplasticity, and loss of PFC density. These may be linked to actin and cytoskeletal regulation, which are enriched throughout the time course.

4.4. Limitations

First, only male mice were studied. Our results lack female methylation responses to chronic pain development, especially important given known sex differences in pain processing.[61] Second, our experiment focused on promoter region methylation, potentially missing DNA methylation regulation in non-promoter regions. DNA methylation in the first intron of coding genes or gene body can affect gene expression.[3,72] Moreover, DNA methylation does not have a linear relationship to gene expression, with other regulatory processes such as RNA transcription or protein translation involved, thus requiring future analysis of gene expression. Third, our tissue samples are derived from whole brain tissue homogenates, and are therefore mixtures of different brain cell types, each with their own cell type-specific profiles of DNA methylation. Thus, the differential methylation signal may be diluted by conflicting methylomic data. Although the lack of significant changes in the proportions of neurons, astrocytes, and microglia mitigates this limitation (**Fig. 2**), changes in other nonneuronal cell types (eg, oligodendrocytes, vascular cells) are not accounted for in the current study. Fourth, the alpha threshold was set at an FDR of 0.1 in this study. It is acknowledged that the selection of an FDR threshold of 0.1 carries a greater risk of type I error (false positive), but is preferable for the exploratory purposes of this study where type II error (false negative) is a greater concern. We recognize these limitations and present these results as a first step towards understanding the epigenetic reprogramming associated with the development and maintenance of chronic pain.

5. Conclusions

Our findings provide evidence for rapid epigenetic reprogramming in the PFC methylome in response to peripheral nerve injury. Thus, epigenetic reprogramming precedes rather than follows chronic pain, consistent with a causal role. Reprograming persists as pain becomes chronic, thereby suggesting an important role for DNA methylation in the initiation, progression, and maintenance of chronic pain. Although some changes in DNA methylation were persistent, dynamic reprogramming was also observed. These patterns may reflect underlying differences

between acute, subchronic and chronic pain, suggesting that therapeutic interventions may have efficacy dependent on pain duration. Pathway analysis revealed enrichment in genes related to stimulus response at early time points, immune function at later time points, and actin and cytoskeletal regulation throughout the time course. These findings highlight the importance of understanding the time course of acute to chronic pain and suggesting broader pain interventions than single gene or protein targets are required.

Conflict of interest statement

L. Stone reports grants from Canadian Institutes for Health Research, during the conduct of the study. The remaining authors have no conflicts of interest to declare.

Appendix A. Supplemental digital content

Supplemental digital content associated with this article can be found online at http://links.lww.com/PAIN/B21, http://links.lww.com/PAIN/B22, http://links.lww.com/PAIN/B27, http://links.lww.com/PAIN/B23, http://links.lww.com/PAIN/B24, http://links.lww.com/PAIN/B25 and http://links.lww.com/PAIN/B26.

References

[1] Alvarado S, Tajerian M, Millecamps M, Suderman M, Stone LS, Szyf M. Peripheral nerve injury is accompanied by chronic transcriptome-wide changes in the mouse prefrontal cortex. Mol Pain 2013;9:21.

[2] Amemiya HM, Kundaje A, Boyle AP. The ENCODE blacklist: identification of problematic regions of the genome. Scientific Rep 2019;9:9354.

[3] Anastasiadi D, Esteve-Codina A, Piferrer F. Consistent inverse correlation between DNA methylation of the first intron and gene expression across tissues and species. Epigenetics Chromatin 2018;11:37.

[4] Apkarian AV, Bushnell MC, Treede RD, Zubieta JK. Human brain mechanisms of pain perception and regulation in health and disease. Eur J Pain 2005;9:463–84.

[5] Apkarian AV, Sosa Y, Sonty S, Levy RM, Harden RN, Parrish TB, Gitelman DR. Chronic back pain is associated with decreased prefrontal and thalamic gray matter density. J Neurosci 2004;24:10410–15.

[6] Baliki MN, Chialvo DR, Geha PY, Levy RM, Harden RN, Parrish TB, Apkarian AV. Chronic pain and the emotional brain: specific brain activity associated with spontaneous fluctuations of intensity of chronic back pain. J Neurosci 2006;26:12165.

[7] Bolger AM, Lohse M, Usadel B. Trimmomatic: a flexible trimmer for Illumina sequence data. Bioinformatics 2014;30:2114–20.

[8] Bourgey M, Dali R, Eveleigh R, Chen KC, Letourneau L, Fillon J, Michaud M, Caron M, Sandoval J, Lefebvre F, Leveque G, Mercier E, Bujold D, Marquis P, Van PT, Anderson de, Lima Morais D, Shao X, Henrion E, Gonzalez E, Quirion P-O, Caron B, Bourque G. GenPipes: an open-source framework for distributed and scalable genomic analyses. Gigascience. 2019;8:giz037.

[9] Bult CJ, Blake JA, Smith CL, Kadin JA, Richardson JE. The mouse genome database G. Mouse genome database (MGD) 2019. Nucleic Acids Res 2018;47:D801–6.

[10] Bushnell MC, Čeko M, Low LA. Cognitive and emotional control of pain and its disruption in chronic pain. Nat Rev Neurosci 2013;14:502–11.

[11] Chaplan SR, Bach FW, Pogrel JW, Chung JM, Yaksh TL. Quantitative assessment of tactile allodynia in the rat paw. J Neurosci Methods 1994; 53:55–63.

[12] Chapman CR, Vierck CJ. The transition of acute postoperative pain to chronic pain: an integrative overview of research on mechanisms. J Pain 2017;18:359.e351–359.e338.

[13] Chen Y, Pal B, Visvader JE, Smyth GK. Differential methylation analysis of reduced representation bisulfite sequencing experiments using edgeR. F1000Res 2017;6:2055.

[14] Decosterd I, Woolf CJ. Spared nerve injury- an animal model of persistent peripheral neuropathic pain. PAIN 2000;87:149–58.

[15] Deval E, Noël J, Lay N, Alloui A, Diochot S, Friend V, Jodar M, Lazdunski M, Lingueglia E. ASIC3, a sensor of acidic and primary inflammatory pain. EMBO J 2008;27:3047–55.

[16] Dina OA, McCarter GC, de Coupade C, Levine JD. Role of the sensory neuron cytoskeleton in second messenger signaling for inflammatory pain. Neuron 2003;39:613–24.

[17] Edgar R, Domrachev M, Lash AE. Gene Expression Omnibus: NCBI gene expression and hybridization array data repository. Nucleic Acids Res 2002;30:207–10.

[18] Faber CG, Lauria G, Merkies IS, Cheng X, Han C, Ahn HS, Persson AK, Hoeijmakers JG, Gerrits MM, Pierro T, Lombardi R, Kapetis D, Dib-Hajj SD, Waxman SG. Gain-of-function Nav1.8 mutations in painful neuropathy. Proc Natl Acad Sci U S A 2012;109:19444–9.

[19] Fuks F. DNA methylation and histone modifications: teaming up to silence genes. Curr Opin Genet Development 2005;15:490–5.

[20] Garriga J, Laumet G, Chen SR, Zhang Y, Madzo J, Issa JPJ, Pan HL, Jelinek J. Nerve injury-induced chronic pain is associated with persistent DNA methylation reprogramming in dorsal root ganglion. J Neurosci 2018;38:6090.

[21] Goldberg DS, McGee SJ. Pain as a global public health priority. BMC Public Health 2011;11:770.

[22] Gölzenleuchter M, Kanwar R, Zaibak M, Al Saiegh F, Hartung T, Klukas J, Smalley RL, Cunningham JM, Figueroa ME, Schroth GP, Therneau TM, Banck MS, Beutler AS. Plasticity of DNA methylation in a nerve injury model of pain. Epigenetics 2015;10:200–12.

[23] Gregoire S, Millecamps M, Naso L, Do Carmo S, Cuello AC, Szyf M, Stone LS. Therapeutic benefits of the methyl donor S-adenosylmethionine on nerve injury-induced mechanical hypersensitivity and cognitive impairment in mice. PAIN 2016;158: 802–10.

[24] Hansson E. Actin filament reorganization in astrocyte networks is a key functional step in neuroinflammation resulting in persistent pain: novel findings on Network restoration. Neurochem Res 2015;40:372–9.

[25] Hess A, Axmann R, Rech J, Finzel S, Heindl C, Kreitz S, Sergeeva M, Saake M, Garcia M, Kollias G, Straub RH, Sporns O, Doerfler A, Brune K, Schett G. Blockade of TNF-α rapidly inhibits pain responses in the central nervous system. Proc Natl Acad Sci 2011;108:3731.

[26] Inquimbert P, Moll M, Latremoliere A, Tong CK, Whang J, Sheehan GF, Smith BM, Korb E, Athié MCP, Babaniyi O, Ghasemlou N, Yanagawa Y, Allis CD, Hof PR, Scholz J. NMDA receptor activation underlies the loss of spinal dorsal horn neurons and the transition to persistent pain after peripheral nerve injury. Cel Rep 2018;23:2678–89.

[27] Iyengar S, Ossipov MH, Johnson KW. The role of calcitonin gene-related peptide in peripheral and central pain mechanisms including migraine. PAIN 2017;158:543–59.

[28] Jackson T, Thomas S, Stabile V, Han X, Shotwell M, McQueen K. Prevalence of chronic pain in low-income and middle-income countries: a systematic review and meta-analysis. Lancet 2015;385:S10.

[29] Jones KD, Gelbart T, Whisenant TC, Waalen J, Mondala TS, Iklé DN, Salomon DR, Bennett RM, Kurian SM. Genome-wide expression profiling in the peripheral blood of patients with fibromyalgia. Clin Exp Rheumatol 2016;34(2 suppl 96):S89–98.

[30] Kanzaki H, Mizobuchi S, Obata N, Itano Y, Kaku R, Tomotsuka N, Nakajima H, Ouchida M, Nakatsuka H, Maeshima K, Morita K.

[31] Kaut O, Schmitt I, Hofmann A, Hoffmann P, Schlaepfer TE, Wüllner U, Hurlemann R. Aberrant NMDA receptor DNA methylation detected by epigenome-wide analysis of hippocampus and prefrontal cortex in major depression. Eur Arch Psychiatry Clin Neurosci 2015;265: 331–41.

[32] Klose RJ, Bird AP. Genomic DNA methylation: the mark and its mediators. Trends Biochem Sci 2006;31:89–97.

[33] Koenigs M, Grafman J. The functional neuroanatomy of depression: distinct roles for ventromedial and dorsolateral prefrontal cortex. Behav Brain Res 2009;201:239–43.

[34] Krueger F, Andrews SR. Bismark: a flexible aligner and methylation caller for Bisulfite-Seq applications. Bioinformatics 2011;27:1571–2.

[35] Kuchinad A, Schweinhardt P, Seminowicz DA, Wood PB, Chizh BA, Bushnell MC. Accelerated brain gray matter loss in fibromyalgia patients: premature aging of the brain? J Neurosci 2007;27:4004.

[36] Kucyi A, Davis KD. The dynamic pain connectome. Trends Neurosciences 2015;38:86–95.

[37] LaCroix-Fralish ML, Ledoux JB, Mogil JS. ThePain Genes Database: an interactive web browser of pain-related transgenic knockout studies. PAIN 2007;131:3e1–3e4.

[38] Leung L, Cahill CM. TNF-α and neuropathic pain—a review. J Neuroinflammation 2010;7:27.

[39] Liu XJ, Liu T, Chen G, Wang B, Yu XL, Yin C, Ji RR. TLR signaling adaptor protein MyD88 in primary sensory neurons contributes to persistent inflammatory and neuropathic pain and neuroinflammation. Scientific Rep 2016;6:28188.

[40] Maiarù M, Tochiki KK, Cox MB, Annan LV, Bell CG, Feng X, Hausch F, Géranton SM. The stress regulator FKBP51 drives chronic pain by modulating spinal glucocorticoid signaling. Sci Translational Med 2016;8: 325ra319.

[41] Marrone MC, Morabito A, Giustizieri M, Chiurchiù V, Leuti A, Mattioli M, Marinelli S, Riganti L, Lombardi M, Murana E, Totaro A, Piomelli D, Ragozzino D, Oddi S, Maccarrone M, Verderio C, Marinelli S. TRPV1 channels are critical brain inflammation detectors and neuropathic pain biomarkers in mice. Nat Commun 2017;8:15292.

[42] Marsch R, Foeller E, Rammes G, Bunck M, Kossl M, Holsboer F, Zieglgansberger W, Landgraf R, Lutz B, Wotjak CT. Reduced anxiety, conditioned fear, and hippocampal long-term potentiation in transient receptor potential vanilloid type 1 receptor-deficient mice. J Neurosci 2007;27:832–9.

[43] Massart R, Dymov S, Millecamps M, Suderman M, Gregoire S, Koenigs K, Alvarado S, Tajerian M, Stone LS, Szyf M. Overlapping signatures of chronic pain in the DNA methylation landscape of prefrontal cortex and peripheral T cells. Sci Rep 2016;6:19615.

[44] Matthews EA, Wood JN, Dickenson AH. Na(v) 1.8-null mice show stimulus-dependent deficits in spinal neuronal activity. Mol Pain 2006;2:5.

[45] McLatchie LM, Fraser NJ, Main MJ, Wise A, Brown J, Thompson N, Solari R, Lee MG, Foord SM. RAMPs regulate the transport and ligand specificity of the calcitonin-receptor-like receptor. Nature 1998;393:333–9.

[46] Meaney MJ, Szyf M. Environmental programming of stress responses through DNA methylation: life at the interface between a dynamic environment and a fixed genome. Dialogues Clin Neurosci 2005;7:103–23.

[47] Meloto CB, Benavides R, Lichtenwalter RN, Wen X, Tugarinov N, Zorina-Lichtenwalter K, Chabot-Dore AJ, Piltonen MH, Cattaneo S, Verma V, Klares R III, Khoury S, Parisien M, Diatchenko L. Human pain genetics database: a resource dedicated to human pain genetics research. PAIN 2018;159:749–63.

[48] Metz AE, Yau HJ, Centeno MV, Apkarian AV, Martina M. Morphological and functional reorganization of rat medial prefrontal cortex in neuropathic pain. Proc Natl Acad Sci 2009;106:2423.

[49] Mifflin KA, Kerr BJ. The transition from acute to chronic pain: understanding how different biological systems interact. Can J Anesthesia 2014;61:112–22.

[50] Millecamps M, Centeno MV, Berra HH, Rudick CN, Lavarello S, Tkatch T, Apkarian AV. D-cycloserine reduces neuropathic pain behavior through limbic NMDA-mediated circuitry. PAIN 2007;132:108–23.

[51] Myers-Schulz B, Koenigs M. Functional anatomy of ventromedial prefrontal cortex: implications for mood and anxiety disorders. Mol Psychiatry 2012;17:132–41.

[52] Nestler EJ. Epigenetic mechanisms of drug addiction. Neuropharmacology 2014;76:259–68.

[53] Paxinos G, Franklin KB. Paxinos and Franklin's the mouse brain in stereotaxic coordinates. Amsterdam, Netherlands: Academic Press, 2019.

[54] Phillips CJ, Harper C. The economics associated with persistent pain. Curr Opin Support Palliat Care 2011;5:127–30.

Expression changes of the neuregulin 1 isoforms in neuropathic pain model rats. Neurosci Lett 2012;508:78–83.

[55] Sanchez-Mut JV, Heyn H, Vidal E, Moran S, Sayols S, Delgado-Morales R, Schultz MD, Ansoleaga B, Garcia-Esparcia P, Pons-Espinal M, de Lagran MM, Dopazo J, Rabano A, Avila J, Dierssen M, Lott I, Ferrer I, Ecker JR, Esteller M. Human DNA methylomes of neurodegenerative diseases show common epigenomic patterns. Translational Psychiatry 2016;6:e718.

[56] Schindelin J, Arganda-Carreras I, Frise E, Kaynig V, Longair M, Pietzsch T, Preibisch S, Rueden C, Saalfeld S, Schmid B, Tinevez J-Y, White DJ, Hartenstein V, Eliceiri K, Tomancak P, Cardona A. Fiji: an open-source platform for biological-image analysis. Nat Methods 2012;9:676.

[57] Schmidt-Wilcke T, Leinisch E, Gänßbauer S, Draganski B, Bogdahn U, Altmeppen J, May A. Affective components and intensity of pain correlate with structural differences in gray matter in chronic back pain patients. PAIN 2006;125:89–97.

[58] Scott KM, Bruffaerts R, Tsang A, Ormel J, Alonso J, Angermeyer MC, Benjet C, Bromet E, de Girolamo G, de Graaf R, Gasquet I, Gureje O, Haro JM, He Y, Kessler RC, Levinson D, Mneimneh ZN, Oakley Browne MA, Posada-Villa J, Stein DJ, Takeshima T, Von Korff M. Depression–anxiety relationships with chronic physical conditions: results from the World Mental Health surveys. J Affective Disord 2007;103:113–20.

[59] Seminowicz DA, Laferriere AL, Millecamps M, Yu JS, Coderre TJ, Bushnell MC. MRI structural brain changes associated with sensory and emotional function in a rat model of long-term neuropathic pain. Neuroimage 2009;47:1007–14.

[60] Shields SD, Eckert WA, Basbaum AI. Spared nerve injury model of neuropathic pain in the mouse- a behavioral and anatomic analysis. J Pain 2003;4:465–70.

[61] Sorge RE, Totsch SK. Sex differences in pain. J Neurosci Res 2017;95: 1271–81.

[62] Strickland IT, Martindale JC, Woodhams PL, Reeve AJ, Chessell IP, McQueen DS. Changes in the expression of NaV1.7, NaV1.8 and NaV1.9 in a distinct population of dorsal root ganglia innervating the rat knee joint in a model of chronic inflammatory joint pain. Eur J Pain 2008;12:564–72.

[63] Tajerian M, Alvarado S, Millecamps M, Vachon P, Crosby C, Bushnell MC, Szyf M, Stone LS. Peripheral nerve injury is associated with chronic, reversible changes in global DNA methylation in the mouse prefrontal cortex. PLoS One 2013;8:e55259.

[64] Tan AM, Samad OA, Fischer TZ, Zhao P, Persson AK, Waxman SG. Maladaptive dendritic spine remodeling contributes to diabetic neuropathic pain. J Neurosci 2012;32:6795.

[65] Tan AM, Stamboulian S, Chang YW, Zhao P, Hains AB, Waxman SG, Hains BC. Neuropathic pain memory is maintained by rac1-regulated dendritic spine remodeling after spinal cord injury. J Neurosci 2008;28: 13173.

[66] Ultsch A, Kringel D, Kalso E, Mogil JS, Lotsch J. A data science approach to candidate gene selection of pain regarded as a process of learning and neural plasticity. PAIN 2016;157:2747–57.

[67] Wang G, Dai D, Chen X, Yuan L, Zhang A, Lu Y, Zhang P. Upregulation of neuregulin-1 reverses signs of neuropathic pain in rats. Int J Clin Exp Pathol 2014;7:5916–21.

[68] Weber M, Hellmann I, Stadler MB, Ramos L, Pääbo S, Rebhan M, Schübeler D. Distribution, silencing potential and evolutionary impact of promoter DNA methylation in the human genome. Nat Genet 2007;39: 457.

[69] Wendt J, Rosenbaum H, Richmond TA, Jeddeloh JA, Burgess DL. Targeted bisulfite sequencing using the SeqCap Epi enrichment system. Methods Mol Biol 2018;1708:383–405.

[70] Wiech K, Kalisch R, Weiskopf N, Pleger B, Stephan KE, Dolan RJ. Anterolateral prefrontal cortex mediates the analgesic effect of expected and perceived control over pain. J Neurosci 2006;26:11501.

[71] Xiao HS, Huang QH, Zhang FX, Bao L, Lu YJ, Guo C, Yang L, Huang WJ, Fu G, Xu SH, Cheng XP, Yan Q, Zhu ZD, Zhang X, Chen Z, Han ZG, Zhang X. Identification of gene expression profile of dorsal root ganglion in the rat peripheral axotomy model of neuropathic pain. Proc Natl Acad Sci 2002; 99:8360.

[72] Yang X, Han H, De Carvalho Daniel D, Lay Fides D, Jones Peter A, Liang G. Gene body methylation can alter gene expression and is a therapeutic target in cancer. Cancer Cell 2014;26:577–90.

[73] Yu G, Wang LG, He QY. ChIPseeker: an R/Bioconductor package for ChIP peak annotation, comparison and visualization. Bioinformatics 2015;31:2382–3.

[74] Zheng W, Xie W, Zhang J, Strong JA, Wang L, Yu L, Xu M, Lu L. Function of gamma-aminobutyric acid receptor/channel rho 1 subunits in spinal cord. J Biol Chem 2003;278:48321–9.

[75] Zhou Y, Zhou B, Pache L, Chang M, Khodabakhshi AH, Tanaseichuk O, Benner C, Chanda SK. Metascape provides a biologist-oriented resource for the analysis of systems-level datasets. Nat Commun 2019;10:1523.

[76] Zimmermann M. Ethical guidelines for investigations of experimental pain in conscious animals. PAIN 1983;16:109–10.